



저작자표시-비영리-변경금지 2.0 대한민국

이용자는 아래의 조건을 따르는 경우에 한하여 자유롭게

- 이 저작물을 복제, 배포, 전송, 전시, 공연 및 방송할 수 있습니다.

다음과 같은 조건을 따라야 합니다:



저작자표시. 귀하는 원저작자를 표시하여야 합니다.



비영리. 귀하는 이 저작물을 영리 목적으로 이용할 수 없습니다.



변경금지. 귀하는 이 저작물을 개작, 변형 또는 가공할 수 없습니다.

- 귀하는, 이 저작물의 재이용이나 배포의 경우, 이 저작물에 적용된 이용허락조건을 명확하게 나타내어야 합니다.
- 저작권자로부터 별도의 허가를 받으면 이러한 조건들은 적용되지 않습니다.

저작권법에 따른 이용자의 권리는 위의 내용에 의하여 영향을 받지 않습니다.

이것은 [이용허락규약\(Legal Code\)](#)을 이해하기 쉽게 요약한 것입니다.

[Disclaimer](#)

Therapeutic effect of periostin-binding DNA aptamer on
autosomal dominant polycystic kidney disease

Chan-Young Jung

The Graduate School
Yonsei University
Department of Medicine

Therapeutic effect of periostin-binding DNA aptamer on autosomal dominant polycystic kidney disease

A Dissertation Submitted
to the Department of Medicine
and the Graduate School of Yonsei University
in partial fulfillment of the
requirements for the degree of
Doctor of Philosophy in Medical Science

Chan-Young Jung

June 2024

**This certifies that the Dissertation
of Chan-Young Jung is approved.**

Thesis Supervisor Jung Tak Park

Thesis Committee Member Shin-Wook Kang

Thesis Committee Member Byung Ha Chung

Thesis Committee Member Beom Jin Lim

Thesis Committee Member Heon Yung Gee

**The Graduate School
Yonsei University
June 2024**

ACKNOWLEDGEMENTS

I would like to express my sincerest gratitude to my supervisor, Professor Jung Tak Park, for his enduring patience and steadfast faith in me. Words fall short of capturing the depth of my appreciation for his mentorship, guidance, and support. His constant encouragement and sage advice were instrumental in the completion of my thesis and dissertation. His invaluable guidance has been a guiding light throughout my journey into nephrology.

I am deeply indebted to Professor Shin-Wook Kang, the esteemed chairman of my thesis committee, and my greatest mentor. His enduring support and encouragement have been fundamental to my development. It is difficult to overstate the impact of his invaluable guidance on my professional journey; without him, I would not have achieved my current standing. I am deeply thankful for his steadfast guidance, wisdom, and invaluable advice, which have been pivotal in inspiring me to excel as a clinician, researcher, and educator, embodying competence, skill, and compassion.

I would also like to thank my thesis committee: Professor Byung Ha Chung, Professor Beom Jin Lim, and Professor Heon Yung Gee, for their insightful comments and thoughtful considerations that helped me further develop and refine my thesis. I extend my sincere gratitude to Professor Young Su Joo, Professor Hyung Woo Kim, Professor Seung

Hyeok Han, and Professor Tae-Hyun Yoo, for their endless support and generosity in sharing their experiences as a clinician, researcher, and teacher. I would also like to express my heartfelt gratitude to Professor Jai Won Chang, and Professor Soon Bae Kim, for their devoted teaching, sincere guidance, and their gracious approval and support of my absences from the clinic, enabling me to advance my thesis work. I would also like to sincerely thank Dr. Bo Young Nam, for her generous assistance and technical expertise in the laboratory. I would also like to show my appreciation to Ms. Hyojung Um, for her administrative support.

I am deeply and sincerely grateful to my parents and parents-in-law, for their endless love, support, and wisdom. Finally, to my caring, loving, and supportive wife, Kijung Choi: my deepest gratitude. This journey would not have been possible without her unwavering support, love, and encouragement. Her belief in me, even in moments of doubt, fueled my resolve and inspired my best work. This achievement, while mine in name, is ours together in spirit and effort.

TABLE OF CONTENTS

LIST OF FIGURES	iii
LIST OF TABLES	iii
ABSTRACT IN ENGLISH	iv
1. INTRODUCTION	1
2. MATERIALS AND METHODS	4
2.1. PERIOSTIN-BINDING DNA APTAMER	4
2.2. CELL CULTURE AND TREATMENT OF HK-2 AND WT9-7 CELLS	4
2.3. FLUORESCENCE-ACTIVATED CELL SORTING ANALYSIS OF WT9-7 CELLS ..	5
2.4. CYST MEASUREMENTS	5
2.5. METHYLTHIAZOLETETRAZOLIUM ASSAY	6
2.6. TOTAL RNA EXTRACTION AND REVERSE TRANSCRIPTION	6
2.7. REAL-TIME QUANTITATIVE POLYMERASE CHAIN REACTION	7
2.8. WESTERN BLOT ANALYSIS	8
2.9. ANIMAL STUDY AND TREATMENT	9
2.10. PERIODIC ACID-SCHIFF STAIN	10
2.11. STATISTICAL ANALYSIS	11
3. RESULTS	12
3.1. CONFIRMATION OF DNA APTAMER BINDING TO PERIOSTIN IN WT9-7 CELLS AND ITS EFFECT ON CELL VIABILITY	12
3.2. PERIOSTIN-BINDING DNA APTAMER ATTENUATES FIBROSIS IN WT9-7 CELLS	14
3.3. PERIOSTIN-BINDING DNA APTAMER TREATMENT ABROGATES CYST GROWTH IN WT9-7 CELLS	17
3.4. PERIOSTIN-BINDING DNA APTAMER TREATMENT ATTENUATES INTEGRIN- LINKED KINASE PATHWAY ACTIVATION IN WT9-7 CELLS	19
3.5. KIDNEY CYST GROWTH IN <i>PKD1</i> SYSTEMIC-KNOCKOUT MICE	21
3.6. PERIOSTIN-BINDING DNA APTAMER TREATMENT AMELIORATES CYST GROWTH AND FIBROSIS IN <i>PKD1</i> SYSTEMIC-KNOCKOUT MICE	24
3.7. PERIOSTIN-BINDING DNA APTAMER TREATMENT ATTENUATES INTEGRIN- LINKED KINASE PATHWAY ACTIVATION IN <i>PKD1</i> SYSTEMIC-KNOCKOUT MICE KIDNEYS	28

4. DISCUSSION	30
5. CONCLUSION	34
REFERENCES	35
ABSTRACT IN KOREAN	43

LIST OF FIGURES

<Fig 1> Specific attachment of a periostin-binding DNA aptamer to periostin expressed in WT9-7 cells and its effect on cell viability.....	13
<Fig 2> mRNA and protein expressions of fibrosis-related molecules are attenuated by periostin-binding DNA aptamer treatment in WT9-7 cells.....	15
<Fig 3> Periostin-binding DNA aptamer treatment ameliorates cell growth in WT9-7 cells.....	18
<Fig 4> Periostin-binding DNA aptamer treatment attenuates ILK pathway activation in WT9-7 cells.....	20
<Fig 5> Kidney size, function, and mRNA and protein expression levels of fibrosis-related molecules in <i>PKDI</i> systemic-knockout mice.....	22
<Fig 6> Periostin-binding DNA aptamer treatment ameliorates kidney cyst growth and attenuates fibrosis-related molecule expressions in <i>PKDI</i> systemic-knockout mice.....	25
<Fig 7> Periostin-binding DNA aptamer treatment attenuates ILK pathway activation in <i>PKDI</i> systemic-knockout mice kidneys.....	29

LIST OF TABLES

<Table 1> Primer sequences.....	8
---------------------------------	---

ABSTRACT

Therapeutic effect of periostin-binding DNA aptamer on autosomal dominant polycystic kidney disease

Background: Autosomal dominant polycystic kidney disease (ADPKD) is a genetically inherited disease in which the kidney generates multiple cysts, eventually leading to decline in kidney function. Periostin, a matricellular protein, is highly overexpressed in cyst-lining epithelial cells of ADPKD compared with normal tubule cells. Periostin accumulates in the extracellular matrix adjacent to ADPKD cysts, binds to the $\alpha V/\beta 3$, $\alpha V/\beta 5$ integrin ligand, and upregulates the protein kinase B (AKT)/mammalian target of rapamycin (mTOR) pathway via activation of the integrin-linked kinase (ILK). Aptamers are oligonucleotides that have the ability to inhibit the activity of specific target proteins by binding to proteins. In this study, the therapeutic effect of periostin-binding DNA aptamer (PA) in ADPKD was investigated.

Methods: *In vitro*, WT9-7 cells treated with PA were evaluated for changes in mRNA and protein expression levels of periostin and fibrosis-related molecules, and changes in the degree of ILK pathway activation. Cyst measurements were also performed to compare cyst growth of WT9-7 cells and control treated with PA. *In vivo*, *PKDI* systemic-knockout mice were employed as the ADPKD model. 8-week and 12-week old mice were sacrificed to observe kidney cyst growth. Mice were given intraperitoneal administration of vehicle or PA via intraperitoneal osmotic pumps for a total duration of 4 weeks, starting at postnatal 4 weeks. Changes in cystic disease parameters, expression levels of periostin and fibrosis-related molecules, and changes in the degree of ILK pathway activation after treatment of PA were examined.

Results: In the fluorescence-activated cell sorting analysis, Cy3-labeled PA was shown to successfully bind to WT9-7 cells. Treatment of WT9-7 cells with PA (200 nM) attenuated the mRNA and protein expressions of fibrosis-related molecules that included periostin, fibronectin, and type I collagen, without affecting cell viability. This was mediated by attenuation of the AKT/mTOR signaling pathway activated by ILK in WT9-7 cells, as shown by decreased expressions of phosphorylated-ILK, phosphorylated-AKT, phosphorylated-mTOR, and phosphorylated-ERK

upon treatment of WT9-7 cells with PA. Additionally, PA ameliorated cell growth in WT9-7 cells. *In vivo* studies revealed that morphological cystic changes in the kidneys of ADPKD mice were observed as early as 8 weeks. Treatment of *PKDI* systemic-knockout mice with PA (500 µg/kg/d) for 4 weeks starting at postnatal 4 weeks ameliorated cyst growth and attenuated the expressions of fibrosis-related molecules. These effects were accompanied by attenuation of ILK pathway activation in the kidneys of *PKDI* systemic-knockout mice.

Conclusions: This study provides evidence that periostin acts as a key mediator of cyst proliferation in ADPKD, and treatment with a DNA aptamer that binds specifically to periostin may be considered as a modality to slow cyst growth and fibrosis in ADPKD.

Key words : autosomal dominant polycystic kidney disease; periostin; aptamers, nucleotide; cysts

I. INTRODUCTION

Autosomal dominant polycystic kidney disease (ADPKD) is the fourth leading cause of kidney failure and the most common inherited kidney disease.¹⁻³ ADPKD is characterized by generation of multiple cysts, which grow in size and number. Cyst burden is directly correlated with the progression of kidney function decline, and most patients eventually develop end-stage kidney disease by the sixth decade of life.^{4,5} To date, tolvaptan, a vasopressin 2 receptor antagonist, is the only drug approved for the treatment of ADPKD. Although it has moderate efficacy,⁵ it is a drug not without tolerability and safety issues such as polyuria and the potential for severe liver toxicity.^{2,6}

The pathophysiology of ADPKD involves the mutation of *PKD1* and *PKD2*, genes that encode polycystin-1 and polycystin-2, respectively.⁷ Polycystin-1 and polycystin-2 form a signaling complex implicated in a variety of cell functions, which leads to progressive enlargement of renal cysts that has features similar to neoplasms such as aberrant cell proliferation, disordered extracellular matrix composition and deposition, and increased angiogenesis. The polycystin proteins are also involved in intracellular calcium homeostasis, where the loss of polycystin function leads to decreased intracellular calcium concentration.⁷⁻⁹ This results in the eventual activation of mammalian target of rapamycin (mTOR), which results in the hyperproliferation of renal tubular cells and subsequent production of inflammation and fibrosis-related proteins, and eventual decline in kidney function.¹⁰

Indeed, studies have indicated that mTOR activity is low in the normal human kidney but strongly upregulated in renal cyst-lining epithelial cells in ADPKD.¹¹ Moreover, mTOR inhibition via rapamycin treatment of rodent PKD models not only resulted in inhibition of renal cyst growth, but also induced regression of kidney size, and preservation of kidney function.¹¹⁻¹⁷ This led to the proposal that mTOR inhibitors, such as sirolimus and everolimus, may be used in patients with ADPKD to retard kidney disease progression. Although animal models evaluating the use of mTOR inhibitors have been encouraging, clinical trials investigating the efficacy and safety of these mTOR inhibitors in patients with ADPKD have been largely disappointing.¹⁸⁻²⁰ For example, in two randomized clinical trials evaluating the efficacy and safety of sirolimus and everolimus, although the administration of mTOR inhibitors resulted in lesser increases in kidney parenchymal volume, but they failed to show any benefits in slowing the progression of kidney impairment, and their

administration was associated with higher rates of drug-specific adverse events such as bone marrow suppression, mucositis, dyslipidemia, and peripheral edema.^{18,19}

Recent studies have further elucidated the pathophysiology of ADPKD, revealing that periostin may play an important role in protein kinase B (AKT)/mTOR activation via stimulation of integrin-linked kinase (ILK). Periostin is a matricellular protein secreted by cyst-lining cells in ADPKD that binds to the components of the extracellular matrix (ECM), including type I collagen and fibronectin.²¹⁻²³ Periostin transmits signals from the ECM to the cell by binding to cell surface integrins, resulting in changes in cell adhesion, proliferation, migration, survival, and tissue angiogenesis.²⁴⁻²⁹ In adults, its expression is limited to collagen-rich tissues and in various cancer cells, such as breast, lung, and colon cancer.^{24,25,28,30-34} Although periostin does not stimulate renal cell proliferation in normal renal cells, in ADPKD cells, however, periostin accumulates within the ECM adjacent to cysts upon secretion by ADPKD cyst-lining cells.³⁵ In fact, periostin was found to be one of the most highly differentially expressed genes in human ADPKD cells compared with normal tubule cells.³⁵ Not only do the poorly differentiated renal tubular cells of ADPKD kidneys overproduce periostin, the resultant increase in kidney mass and intracystic pressure also stimulates further production of periostin from the renal tubular cells.³⁶ Periostin binds to the $\alpha V/\beta 3$, $\alpha V/\beta 5$ integrin ligand and stimulates ILK, which triggers acceleration of cell proliferation and *in vitro* cyst growth of ADPKD cells. In a slowly progressive model of renal cystic disease involving *pcy/pcy* mice, knockout of the periostin gene expression not only reduced the number of cysts and cystic area, but also showed a significant reduction in the levels of a key mTOR downstream component, suggesting a potential role of periostin in the activation of the AKT-mTOR signaling axis.³⁶

Insights into the role of periostin in the activation of the periostin-ILK-AKT-mTOR signaling axis have led to further studies involving the inhibition of the integrin pathway. Although pharmacological inhibition or shRNA knockout of ILK in ADPKD cells suppressed AKT/mTOR activation and subsequent cell proliferation, ILK knockout mice eventually developed kidney fibrosis, tubular dilation, apoptosis, and kidney failure by 10 weeks, suggesting that some activity of the ILK pathway may be required for kidney cell survival and epithelium maintenance. However, reduced ILK expression in a rapidly progressive model of ADPKD not only decreased AKT/mTOR activity, cell proliferation and growth, but also showed improved kidney function and survival.³⁷ Furthermore, conditional inactivation of integrin- $\beta 1$ in collecting ducts resulted in inhibition of *PKDI*-dependent cystogenesis with a concomitant suppression of fibrosis and preservation of

kidney function,³⁸ suggesting that drugs that target the integrin signaling pathway may be effective for slowing kidney disease progression in ADPKD.

Aptamers are oligonucleotides composed of DNA or RNA single strands that can bind to specific target proteins. Their ability to inhibit the activity of specific target proteins by their protein-specific binding ability has led to the application of aptamers in various clinical fields.³⁹ Aptamers are produced chemically and have shown to be relatively bio-stable, thus resulting in lower production costs, and more convenient storage and distribution compared to antibodies.⁴⁰ Due to these advantages of aptamers, they have been considered promising drug candidates in various diseases, such as diabetes, human immunodeficiency virus infection, and macular degeneration.⁴⁰⁻⁴² In more recent experimental studies, aptamers that specifically bind to periostin have been shown to not only inhibit breast cancer cell growth and metastasis,⁴³ but they have also been shown to attenuate kidney fibrosis under diabetic conditions,⁴⁴ and suppress peritoneal dialysis-induced peritoneal fibrosis.⁴⁵

Hence, in this study, the therapeutic effect of periostin-binding DNA aptamer (PA) in ADPKD was investigated both *in vitro* and *in vivo*.

II. MATERIALS AND METHODS

2.1. Periostin-binding DNA aptamer

A modified DNA systematic evolution of ligands by exponential enrichment (SELEX) procedure was used to select periostin-specific aptamers.^{43,46} PAs were constructed by Aptamer Sciences Inc. (Pohang, South Korea), as previously reported.⁴³ Sequences of the aptamers used in this study are shown in **Table 1**. Aptamers were prepared in two forms: Cy3-labeled aptamer, and polyethylene glycol (PEG)-conjugated aptamer. The Cy3-labeled PA were prepared by labeling Cy3 to the 5' end of the aptamer. The Cy3-labeled PA was used to evaluate the periostin-specific aptamer attachment in *in vitro* studies. The PEG-conjugated PA was prepared by conjugating 40 kDa PEG to the 5' end, and inverted dT to the 3' end to increase its *in vivo* biological stability. The PEG-conjugated PA was used for *in vivo* studies.

2.2. Cell culture and treatment of HK-2 and WT9-7 cells

Human kidney-2 (HK-2) cells (American Type Culture Collection, Manassas, VA, USA) and WT9-7 cells (American Type Culture Collection, Manassas, VA, USA), an immortalized cell line originally derived from a human ADPKD kidney,⁴⁷ were both cultured at 37°C in a humidified 95% air/5% CO₂ atmosphere in a Minimum Essential Medium (Gibco, Thermo Fisher Scientific, Waltham, MA, USA) supplemented with 10% Fetal bovine serum (FBS) (Sigma-Aldrich, St. Louis, MO, USA), 10,000 U/mL penicillin, and 10,000 µg/mL streptomycin (Gibco, Thermo Fisher Scientific, Waltham, MA, USA). The WT9-7 cells, originated from a non-dilated tubule, possess proximal tubular characteristics. They are heterozygous for a truncating *PKDI* gene (Q2556X) and possess the full-length form of polycystin-1.^{47,48}

For periostin knockdown experiments, periostin siRNA (Dharmacon, Lafayette, CO, USA), negative control scramble siRNA (Dharmacon, Lafayette, CO, USA), and positive control GAPDH siRNA (Bioneer, Daejeon, South Korea) were used. Periostin siRNA was transfected with Lipofectamine 2000 (Invitrogen, Carlsbad, CA, USA) according to the manufacturer's protocol. Briefly, 6 µL of Lipofectamine 2000 was diluted in 1 mL of Opti-MEM I Reduced Serum Medium (Invitrogen, Carlsbad, CA, USA), incubated for 15 min at room temperature (RT), and mixed with

periostin siRNA. After a 15 min incubation at RT, the mixture was added to each well of WT9-7 cells, which were plated at a density of 5×10^5 cells/well into six-well plates the day before, and the medium was changed after 24 h. The doses of periostin siRNA for this study were determined based on preliminary experimental results.

2.3. Fluorescence-activated cell sorting analysis of WT9-7 cells

ADPKD cells were centrifuged at 500 g for 5 min and washed twice in an isotonic, calcium, and magnesium free-phosphate buffered saline (PBS) buffer to remove residual growth factors in the medium. A final concentration of 1×10^7 cells/mL was re-suspended and incubated with 200 nM Cy3-labeled PA containing binding buffer (PBS including 5 mM $MgCl_2$). Samples of 100 μ L were used per assay (1×10^6 cells) into each 1.5 mL tube for staining. Flow cytometric analysis of surface staining intensity was performed using an FACSVERSE System (BD Biosciences, Franklin Lakes, NJ, USA) and signals were obtained from a blue laser. Analysis of the results was conducted using FACSuite software (BD Biosciences, Franklin Lakes, NJ, USA).

2.4. Cyst measurements

The 3D culture was performed using Matrigel matrix (Corning, NY, USA) to assess cyst formation. For cyst formation, WT9-7 cells (1×10^3 cells/well) were trypsinized and resuspended as a single-cell suspension in type I collagen solution and transferred to 24-well plates on preformed Matrigel. The plate was incubated for 15 min at 37°C to promote gelation. Following this, 500 μ L of Dulbecco's Modified Eagle Medium (DMEM) (Gibco, Thermo Fisher Scientific, Waltham, MA, USA) with 20% FBS was added. After cell attachment to the gel, additional Matrigel was added to the cells to form a sandwich-like pattern. Cells were maintained in 3D culture at 37°C and humidified 5% CO_2 . To promote cyst proliferation, 10 μ M forskolin (Sigma-Aldrich, St. Louis, MO, USA), a cyclic adenosine monophosphate agonist, was added to the medium at day 0. After the induction of cyst formation with forskolin, HK-2 and WT9-7 cells were treated with or without 200 nM PA from days 0 to 10, and the medium was changed every 2 days. To quantify cyst growth in response to treatments, between 10–12 images of individual cysts, chosen at random, were obtained at 20 \times magnification from each well on day 10, using the confocal LSM700 Zeiss microscope and

Zeiss camera (Zeiss Microscopy GmbH, Jena, Germany). Diameters of all captured spherical cysts were analyzed using ImageJ software ver. 1.49 (National Institutes of Health, Bethesda, MD, USA; accessible online at <http://imagej.net/ij>).

2.5. Methylthiazoletetrazolium assay

The methylthiazoletetrazolium (MTT) (Abcam, Cambridge, UK) assay is an indicator of the number of metabolically active cells and is therefore a measure of cell viability, proliferation, and cytotoxicity.⁴⁹ To assess the cell cytotoxicity and cell proliferation upon treatment of the WT9-7 cells with PA, WT9-7 cells were cultured in 96-well culture plates. Phenol red-free DMEM with 1 mg/mL of MTT reagent were added to each well after the experimental periods, and then incubated at 37°C for 3 h in humidified 5% CO₂. After incubation, 150 µL of MTT solvent were added to each well. The culture plate was then wrapped in foil, and then shaken on an orbital shaker for 15 min. Optical density (OD) was measured with a microplate reader (SpectraMax 340, Molecular Devices, San Jose, CA, USA) at a wave length of 590 nm. The OD of the control group cells was assigned a relative value of 100. For the assessment of cell cytotoxicity and cell proliferation, cells were incubated with vehicle control (PBS), 10, 100, 200, and 400 nM of PA. Percentage cell cytotoxicity was calculated by $(100 \times (\text{control} - \text{sample})) / \text{control}$. For the assessment of cell proliferation, absorbance was measured at 590 nm to calculate the number of viable cells.

2.6. Total RNA extraction and reverse transcription

For HK-2 and WT9-7 cells, 700 µL of RNAiso reagent (Takara Bio Inc., Kusatsu, Shiga, Japan) were added to the cell culture dish, and the suspension was collected and homogenized for 5 min at room temperature (RT). Kidney samples were rapidly frozen using liquid nitrogen and homogenized by mortar and pestle thrice with 700 µl of RNAiso reagent. 160 µl of chloroform was subsequently added to the homogenized samples of the cells and kidneys. The mixture was then shaken vigorously for 30 s, stored for 3 min at RT, and centrifuged at 12,000 rpm for 15 min at 4°C. Among the separated layers, samples from the aqueous layer was transferred to a fresh tube, precipitated by adding 400 µL of isopropanol, and pelleted by centrifugation at 12,000 rpm for 30 min at 4°C. The RNA precipitate was washed with 70% ethanol, air-dried for 2 min, and dissolved in sterile diethyl

pyrocarbonate-treated distilled water. The quantity and quality of extracted RNA were assessed using spectrophotometric measurements at 260 and 280 nm wavelengths.

A Takara cDNA synthesis kit (Takara Bio Inc., Kusatsu, Shiga, Japan) was used to obtain first strand cDNA. Reverse transcription was conducted using 2 μg of total RNA extracts with 10 μM random hexanucleotide primer, 1 mM dNTP, 8 mM MgCl_2 , 30 mM KCl, 50 mM Tris-HCl at pH 8.5, 0.2 mM dithiothreitol, 25 U RNase inhibitor, and 40 U PrimeScript reverse transcriptase. The mixture was then incubated for 10 min at 30°C, and for 1 h at 42°C, followed by incubation for 5 min at 99°C for enzyme inactivation.

2.7. Real-time quantitative polymerase chain reaction

Using the ABI PRISM 7700 Sequence Detection System (Applied Biosystems, Foster City, CA, USA), a mixture with a total volume of 20 μL , containing 10 μL SYBR Green PCR Master Mix (Applied Biosystems, Foster City, CA, USA), 5 μL of reverse transcribed cDNA, and 5 pmol sense and antisense primers. The primer sequences used in this study are described in **Table 1**. The optimal primer concentrations were determined from the results of preliminary experiments. All polymerase chain reactions started with an initial heating step for 9 min at 95°C, and ended with a final extension for 7 min at 72°C after repetitive cycles. The quantitative real-time polymerase chain reaction (qPCR) was performed under the following conditions: 35 cycles of denaturation for 30 min at 94.5°C, annealing for 30 s at 60°C, and extension for 1 min at 72°C. Each sample was run in triplicate in separate tubes and a control without cDNA was also run in parallel with each assay. After qPCR, the temperature was increased from 60 to 95°C at a rate of 2°C/min to construct a melting curve. The cDNA content of each specimen was determined using a comparative CT method with $2^{-\Delta\Delta\text{CT}}$. The results were given as the relative expression normalized to the expression of 18S rRNA and expressed in arbitrary units.

Table 1. Primer sequences used for real-time qPCR

Genes	Sequence (5' → 3')	
<i>18S</i> (human)	Forward	ACCGCGTTCATTTTGT
	Reverse	CGGTCCAAGAATTCACCTC
<i>Periostin</i> (human)	Forward	GGCACCAAAAAGAAATACT
	Reverse	GGAAGGTAAGAGTATAT
<i>Fibronectin</i> (human)	Forward	AACCTACGGATGACTCGTGC
	Reverse	TGAATCACATCTGAAATGACCAC
<i>Type I collagen</i> (human)	Forward	ACTGGTACATCAGCCCGAAC
	Reverse	TACTCGAACGGGAATCCATC
<i>18S</i> (mouse)	Forward	CGCTTCCTTACCTGGTTGAT
	Reverse	GGCCGTGCGTACTTAGACAT
<i>PKD1</i> (mouse)	Forward	ACCAGAGTGCTGCCATCTTC
	Reverse	TTCATCCGCTCCACAGTGAC
<i>Periostin</i> (mouse)	Forward	GGCACCAAAAAGAAATACT
	Reverse	GGAAGGTAAGAGTATAT
<i>Fibronectin</i> (mouse)	Forward	ACAGAGCTCAACCTCCCTGA
	Reverse	TGTGCTCTCCTGGTTCTCTCT
<i>Type I collagen</i> (mouse)	Forward	TCAATTGCTCCGGCCGCTG
	Reverse	CCAGCGTCTGAAGTAGGTTGTGGG

2.8. Western blot analysis

Expression levels of periostin, fibronectin, type I collagen, β -actin, phosphorylated-ILK, ILK, phosphorylated-AKT, AKT, phosphorylated-mTOR, mTOR, phosphorylated-ERK, and ERK, were examined using Western blot analyses. Protein samples from HK-2 and WT9-7 cells, and harvested kidney tissue from mice were prepared using lysis buffer containing sodium dodecyl sulfate (SDS) sample buffer [2T SDS, 10 mM Tris·HCl, pH 6.8, 10% (vol/vol) glycerol]. Aliquots of protein samples were mixed with Laemmli sample buffer, and then heated at 100°C for 5 min, and subjected to electrophoresis in a 8–12% polyacrylamide denaturing (SDS containing) gel. Proteins were then transferred to a Hybond-ECL membrane in a Hoeffer semidry blotting apparatus (Hoeffer Instruments, San Francisco, CA, USA), and the membrane was then incubated in blocking buffer A [1 × TBS, 0.1% Tween 20, and 5% nonfat milk] for 30 min at RT, followed by an overnight incubation at 4°C with an appropriate dilution of primary antibodies specific to periostin (Abcam, Cambridge, UK), fibronectin (Dako, Glostrup, Denmark), type I collagen (Southern Biotech,

Birmingham, AL, USA), β -actin (Sigma-Aldrich, St. Louis, MO, USA), phosphorylated-ILK (Cell Signaling Technology, Danvers, MA, USA), ILK (Cell Signaling Technology, Danvers, MA, USA), phosphorylated-AKT (Cell Signaling Technology, Danvers, MA, USA), AKT (Cell Signaling Technology, Danvers, MA, USA), phosphorylated-mTOR (Cell Signaling Technology, Danvers, MA, USA), mTOR (Cell Signaling Technology, Danvers, MA, USA), phosphorylated-ERK (Santa Cruz Biotechnology, Santa Cruz, CA, USA), or ERK (Santa Cruz Biotechnology, Santa Cruz, CA, USA). The membranes were washed three times for 10 min in $1 \times$ TBS with 0.1% Tween-20 and incubated in buffer A containing a 1:1,000 dilution of horseradish peroxidase-linked goat anti-rabbit or anti-mouse IgG (Santa Cruz Biotechnology, Santa Cruz, CA, USA). Several washes were done, and the membrane was developed with a chemiluminescent reagent (ECL; Amersham Life Science, Arlington Heights, IL, USA). ImageJ ver. 1.49 (National Institutes of Health, Bethesda, MD, USA; accessible online at <http://imagej.net/ij>) was used to quantify the band intensities. Changes in the optical densities of the bands of the treated groups relative to control cells or tissues were analyzed.

2.9. Animal study and treatment

The protocols for animal experiments were approved by the Committee for the Care and Use of Laboratory Animals at Yonsei University College of Medicine, Seoul, Republic of Korea. Mice were housed in a temperature-controlled room and given access to food and water *ad libitum* throughout the study period. All animal experiments were conducted in accordance with the Principles of Laboratory Animal Care (NIH Publication no. 85-23, revised 1985).

To establish the *PKDI* systemic-knockout mice model, *PKDI* floxed-allele female mouse (Jackson Laboratories, Bar Harbor, ME, USA) and tamoxifen-inducible Cre protein expressing tamoxifen-CreER male mouse (Jackson Laboratories, Bar Harbor, ME, USA) were mated. In order to induce *PKDI* systemic-knockout, adult mice, 3–4 months of age, were treated with 5 mg tamoxifen for three consecutive days, using a feeding needle. Weaning mothers, 3–6 months of age, received a similar treatment starting at postnatal day 4 of the progeny, and these newborn mice received tamoxifen via breast-feeding from the mother. To check for successful *PKDI* gene knock-out, genotypes were assessed by PCR analysis of genomic DNA from mouse toe lysates using the Jackson Laboratory primer (Jackson Laboratories, Bar Harbor, ME, USA).

To observe the morphological changes in *PKDI* systemic-knockout ADPKD mice kidney, 8-

and 12-weeks old mice were sacrificed while anesthetized with Zoletil (10 mg/kg; Virbac, Carros, France). The kidneys were extracted, of which one was used in real-time PCR and Western blot analysis for observation of mRNA and protein expression, respectively, and the other was 10% formalin-fixed, paraffin-embedded, and stained for morphological analysis.

To observe the effects of treatment with PA, all newborn mice were implanted with intraperitoneal osmotic pumps at postnatal 4 weeks for intraperitoneal administration of vehicle (PBS) or PA. The study group was split into four groups. In the wild-type (WT) group, mice were injected with diluent. In the WT + PA group, the PA (500 µg/kg/d) was administered intraperitoneally. In the *PKD* group, mice were injected with vehicle. In the *PKD* + PA group, the PA (500 µg/kg/d) was administered intraperitoneally. The dose of PA was selected based on the protocols of previous studies.^{44,45} Vehicle or PA was administered using an Alzet Model osmotic pump (Durect Corp., Palo Alto, CA, USA) starting at postnatal 4 weeks for 4 weeks before sacrifice. Kidneys of mice were removed and used in real-time PCR and Western blot analysis for observation of mRNA and protein expression, respectively.

2.10. Periodic Acid-Schiff stain

To evaluate the morphological changes of mice kidney tissue, formalin-fixed, paraffin-embedded mice kidney slices were stained with Periodic Acid-Schiff (PAS) (Sigma-Aldrich, St. Louis, MO, USA) dye for routine histological examination. Images were taken with an Olympus DP73 microscope (Olympus Corp., Tokyo, Japan). PAS staining was performed with dissolved paraffin placing the tissue slides in a 60°C incubator for at least 30 min. Subsequently, sequential rehydration process was done with xylene and 100%, 95%, and 90% alcohol. After washing the slides with distilled water for 7 min to soak the periodic acid, the slides were reacted in Schiff's solution for 15 min. Modified Mayer's Hematoxylin counterstaining was performed after the dehydration process. The PAS-stained tissues were used to observe the morphological changes in *PKDI* systemic-knockout ADPKD mice kidney. For percentage cystic area from PAS slides, the perimeters of the sections from digitally acquired images were outlined using the positive selection pen, while excluding the medullary regions. The white and colored areas of the image were derived from the positive pixel count algorithm. For percentage-positive pixels in images, a total of eight 20× fields of view from the kidney cortex were analyzed and averaged for each mouse, using ImageJ

software ver. 1.49 (National Institutes of Health, Bethesda, MD, USA; accessible online at <http://imagej.net/ij>).

2.11. Statistical analysis

Experimental data were analyzed using GraphPad Prism ver. 9.4 (GraphPad Software, San Diego, CA, USA). Data are expressed as means \pm standard errors of mean. One-way analysis of variance (one-way ANOVA) was performed and was followed by the Tukey test and student's *t*-test for multiple and single comparisons, respectively. A *P*-value <0.05 was considered statistically significant.

III. RESULTS

3.1. Confirmation of DNA aptamer binding to periostin in WT9-7 cells and its effect on cell viability

To determine whether the PA attached specifically to periostin, fluorescence-activated cell sorting (FACS) analysis was conducted to demonstrate that the PA attached specifically to periostin in WT9-7 cells. A Cy3-labeled PA was used to evaluate the amount of PA that attached to periostin expressed in WT9-7 cells. Compared to the negative control, WT9-7 cells treated with Cy3-labeled PA showed an increase in the Cy3-positive fraction of the total WT9-7 cell count (88.3%). The Cy3-positive fraction was significantly abrogated (15.4%) by periostin siRNA (100 nM) transfection, suggesting that the PA specifically binds to periostin expressed by WT9-7 cells (**Figure 1A**), without affecting cell viability (**Figure 1B**).

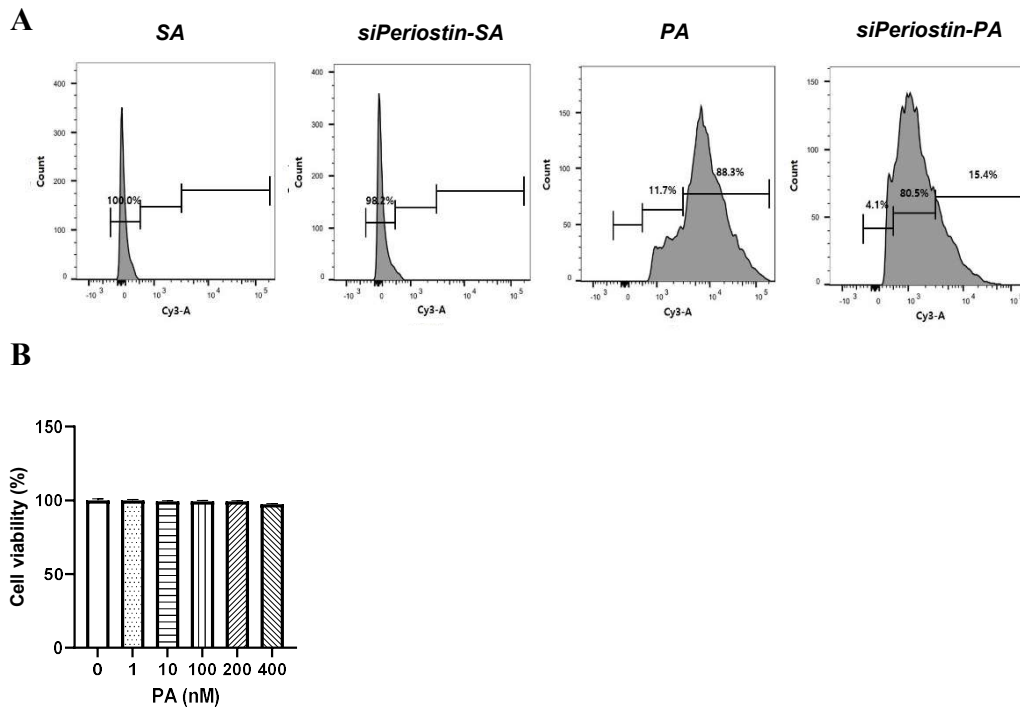


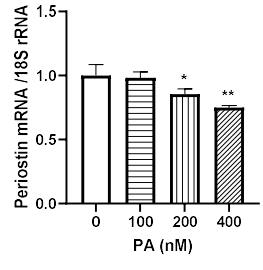
Figure 1. Specific attachment of periostin-binding DNA aptamer to periostin expressed in WT9-7 cells and its effect on cell viability. FACS analysis was performed in WT9-7 cells treated with periostin siRNA (100 nM) and Cy3-labeled PA (200 nM). (A) The Cy3-positive fraction was significantly increased in WT9-7 cells treated with the Cy3-labeled PA, which was significantly abrogated by periostin siRNA transfection. (B) Cell viability following treatment with PA at different doses indicate that cell viability was not affected at different doses of PA.

Abbreviations: SA, negative control scramble aptamer; siPeriostin, periostin siRNA; PA, periostin-binding DNA aptamer; FACS, fluorescence-activated cell sorting.

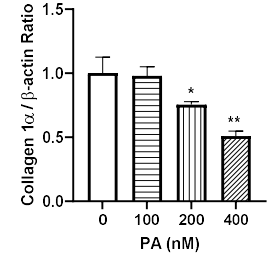
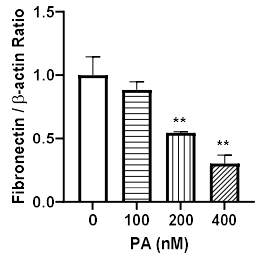
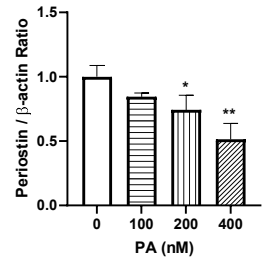
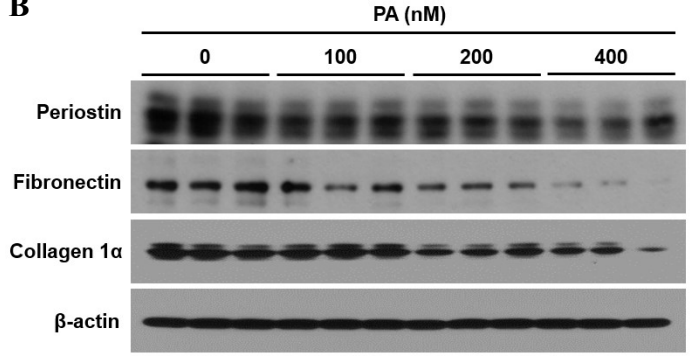
3.2. Periostin-binding DNA aptamer attenuates fibrosis in WT9-7 cells

To determine whether blocking periostin signaling with the PA could attenuate fibrosis in WT9-7 cells, the changes in the expression of periostin and fibrosis-related molecules were examined after treatment of WT9-7 cells with different doses of PA (**Figure 2**). As shown in **Figures 2A** and **2B**, PA (200 and 400 nM) attenuated the mRNA and protein expressions of periostin, fibronectin, and type I collagen. Upregulated mRNA levels of periostin, fibronectin, and type I collagen were significantly attenuated by PA treatment in WT9-7 cells (**Figure 2C**). The increased protein levels of periostin, fibronectin, and type I collagen were also significantly abrogated by PA treatment in WT9-7 cells (**Figure 2D**). These results indicate that PA effectively mitigates fibrosis by inhibiting the expression of periostin and fibrosis-related molecules in ADPKD cells.

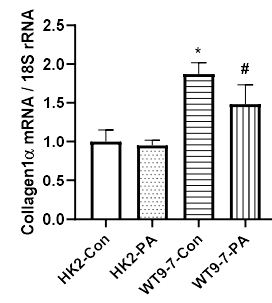
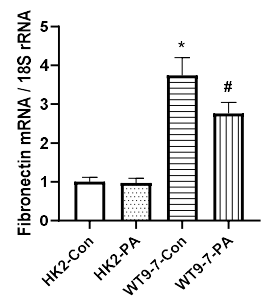
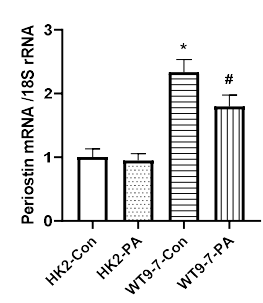
A



B



C



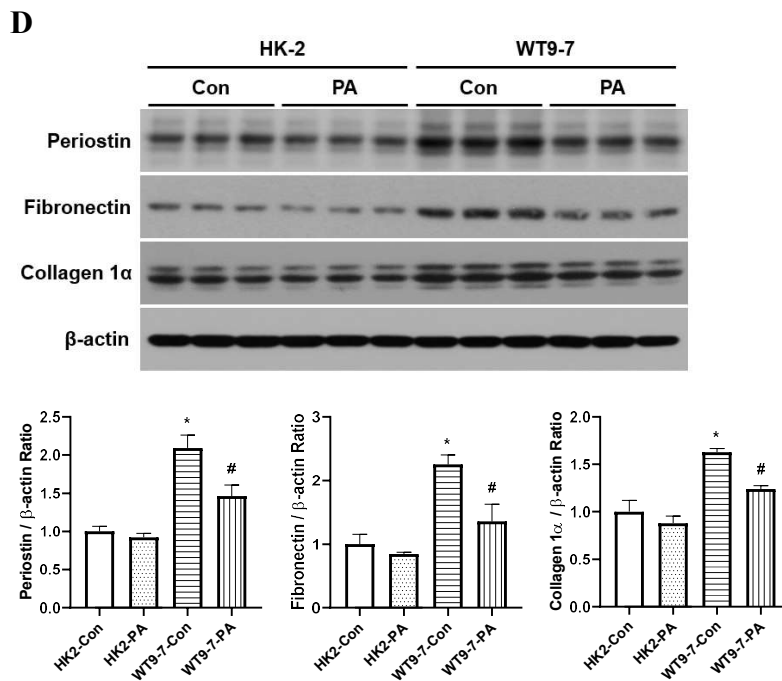


Figure 2. mRNA and protein expressions of fibrosis-related molecules are attenuated by periostin-binding DNA aptamer treatment in WT9-7 cells. (A) Relative mRNA level quantification of periostin, fibronectin, and type I collagen in WT9-7 cells at different concentrations of PA (0, 100, 200, and 400 nM). PA (200 and 400 nM) significantly downregulated mRNA expression levels of periostin, fibronectin, and type I collagen. (B) A representative Western blot analysis of protein expression in WT9-7 cells at different concentrations of PA (0, 100, 200, and 400 nM). PA (200 and 400 nM) significantly attenuated protein expression levels of periostin, fibronectin, and type I collagen. (C) Periostin, fibronectin, and type I collagen mRNA levels. Treatment with PA (200 nM) significantly ameliorated periostin, fibronectin, and type I collagen mRNA expression. (D) A representative Western blot analysis of protein expression in WT9-7 cells with or without PA (200 nM). PA significantly downregulated protein expression levels of periostin, fibronectin, and type I collagen in WT9-7 cells.

Note: *, $P < 0.05$ vs. HK-2 or PA 0 nM; #, $P < 0.05$ vs. WT9-7 control; **, $P < 0.01$ vs. PA 0 nM.

Abbreviations: PA, periostin-binding DNA aptamer; HK-2, human kidney-2; con, control.

3.3. Periostin-binding DNA aptamer treatment abrogates cyst growth in WT9-7 cells

The potential of PA to affect cyst growth in ADPKD cells was assessed using WT9-7 cells and HK-2 cells as control. WT9-7 cells form cysts when cultured in a three-dimensional environment with stimulation by the addition of forskolin promoting cyst swelling. PA significantly inhibited cyst growth of WT9-7 cells by day 10 (**Figures 3A and B**). The mean cyst diameter of WT9-7 cells treated with PA was significantly less than that of the vehicle control. Moreover, as shown in **Figure 3C**, treatment of WT9-7 cells with PA significantly reduced ADPKD cell proliferation compared to vehicle-treated cells. These findings suggest that PA treatment abrogates cyst growth in WT9-7 cells.

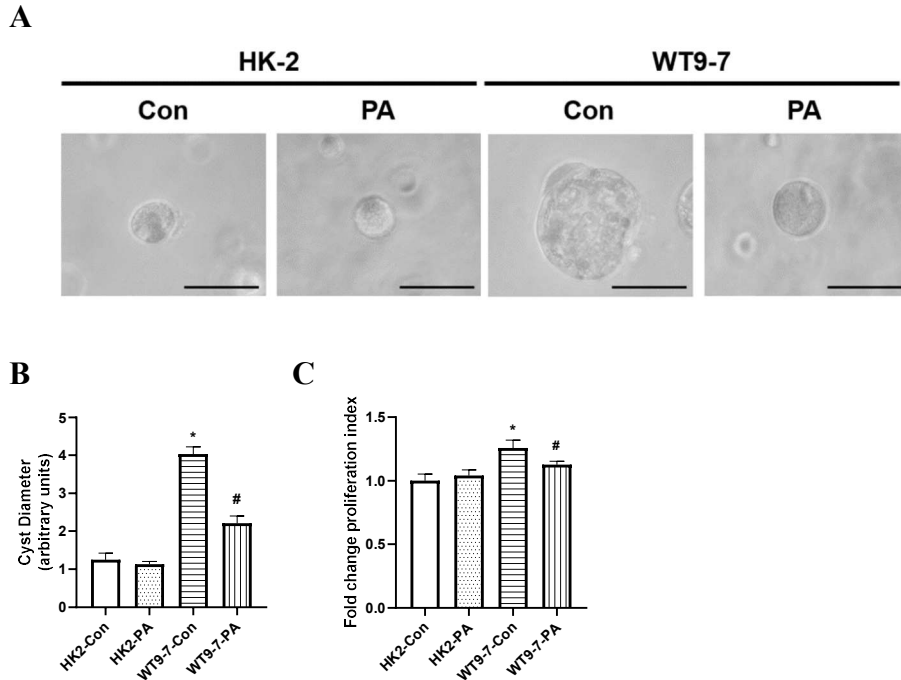


Figure 3. Periostin-binding DNA aptamer treatment ameliorates cell growth in WT9-7 cells. (A) Representative photos show that PA significantly reduced cyst growth in WT9-7 cells at day 10. Bar = 200 μ m. (B) Mean cyst diameter of HK-2 and WT9-7 cells at day 10, treated with either vehicle or PA. The mean cyst diameter of WT9-7 cells treated with PA was significantly less than that of the vehicle control. (C) Effect of PA treatment on cell proliferation in WT9-7 cells. Fold changes in proliferation index were significantly lower in WT9-7 cells treated with PA, compared to vehicle control.

Note: *, $P < 0.05$ vs. HK-2; #, $P < 0.05$ vs. WT9-7 control.

Abbreviations: HK-2, human kidney-2; con, control; PA, periostin-binding DNA aptamer.

3.4. Periostin-binding DNA aptamer treatment attenuates integrin-linked kinase pathway activation in WT9-7 cells

To determine whether the anti-fibrotic effect of PA was mediated by attenuation of the signaling pathway activated by ILK in WT9-7 cells, the changes in the expression of phosphorylated-ILK, phosphorylated-AKT, phosphorylated-mTOR, and phosphorylated-ERK were examined after treatment of WT9-7 cells with PA (**Figure 4**). When the cells were examined for phosphorylated-ILK expression, PA treatment of WT9-7 cells attenuated expression levels of phosphorylated-ILK, normalized to total ILK. Similar findings were observed for phosphorylated-AKT, phosphorylated-mTOR, and phosphorylated-ERK. These results indicate that PA treatment attenuated ILK pathway activation in WT9-7 cells, as shown by the downregulation of downstream components of the ILK pathway.

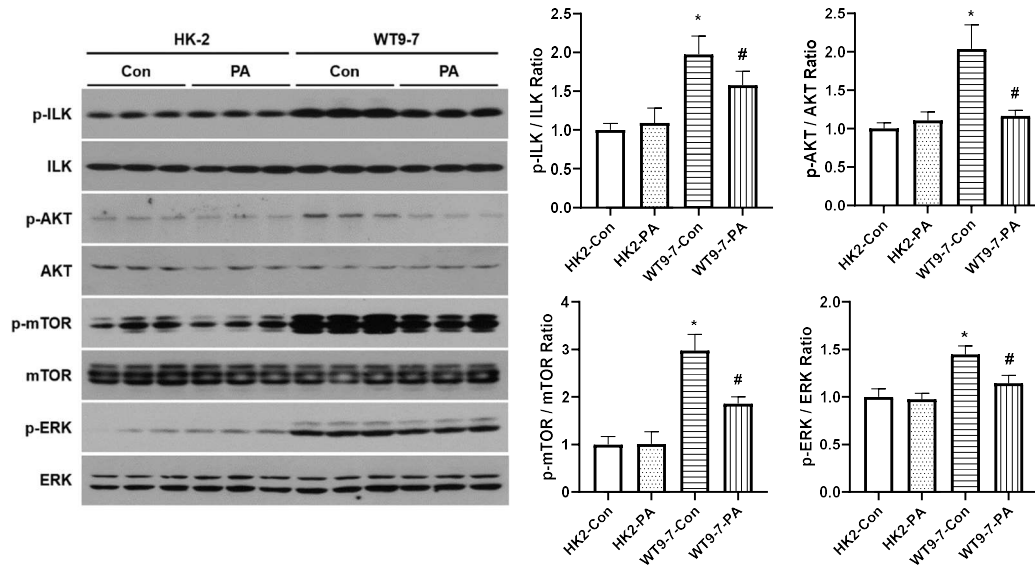


Figure 4. Periostin-binding DNA aptamer treatment attenuates ILK pathway activation in WT9-7 cells. Representative Western blotting analysis of phosphorylated-ILK, phosphorylated-AKT, phosphorylated mTOR, and phosphorylated-ERK. The increases in the protein levels of phosphorylated-ILK, phosphorylated-AKT, phosphorylated mTOR, and phosphorylated-ERK were significantly attenuated by PA, whereas total levels of ILK, AKT, mTOR, and ERK remain unchanged. Quantification of phosphorylated-ILK to ILK ratio (p-ILK/ILK), phosphorylated-AKT to AKT ratio (p-AKT/AKT), phosphorylated-mTOR to mTOR ratio (p-mTOR/mTOR), and phosphorylated-ERK to ERK ratio (p-ERK/ERK) show attenuated expressions upon PA treatment. *Note:* *, $P < 0.05$ vs. HK-2; #, $P < 0.05$ vs. WT9-7 control.

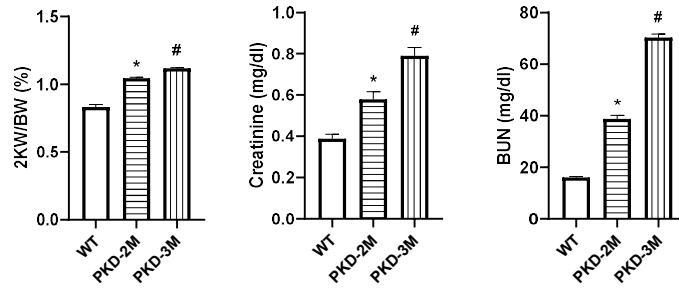
Abbreviations: HK-2, human kidney-2; con, control; PA, periostin-binding DNA aptamer; ILK, integrin-linked kinase; AKT, protein kinase B; mTOR, mammalian target of rapamycin; ERK, extracellular signal-regulated kinase.

3.5. Kidney cyst growth in *PKDI* systemic-knockout mice

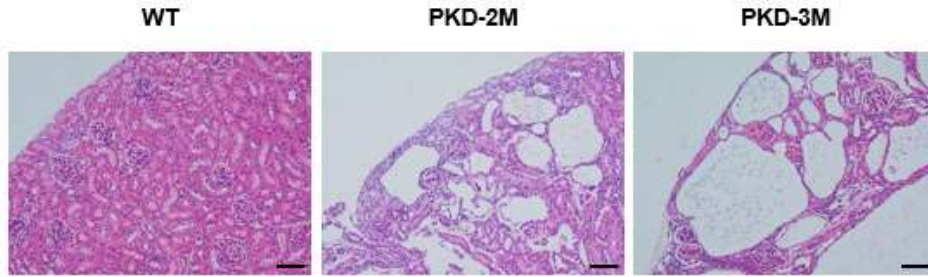
To observe the morphological changes in mouse models of ADPKD, 8-week and 12-week-old mice were sacrificed, and their kidneys were examined. After the 8-week or 12-week experimental period, the kidney and body weights were significantly higher in *PKDI* systemic-knockout mice compared to those of WT mice (**Figure 5A**). In addition, the mean serum creatinine and blood urea nitrogen (BUN) levels were significantly higher in *PKDI* systemic-knockout mice compared to those of WT mice. Kidney and body weight, serum creatinine and BUN levels were significantly higher in 12-week-old *PKDI* systemic-knockout mice compared to those of WT mice.

Histological examination of the kidneys from 2- and 3-months old mice showed rapid progression of polycystic kidney disease (**Figure 5B**), with the morphological cystic changes observed as early as 8 weeks. The calculated cystic indices also significantly increased over time in *PKDI* systemic-knockout mice (**Figure 5C**). When the mRNA and protein expression levels were observed, *PKDI* systemic-knockout mice showed upregulation in levels of periostin and fibrosis-related molecules over time (**Figures 5D and E**). These findings suggest that kidney cyst growth in ADPKD mice is accompanied by accumulation of periostin and fibrosis-related molecules.

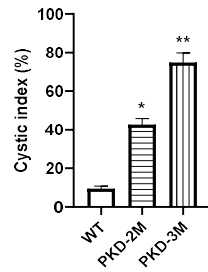
A



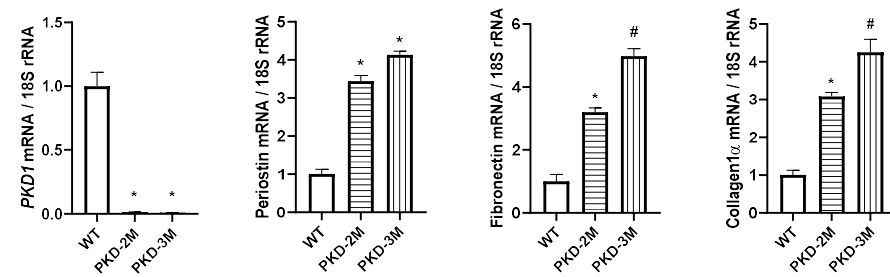
B



C



D



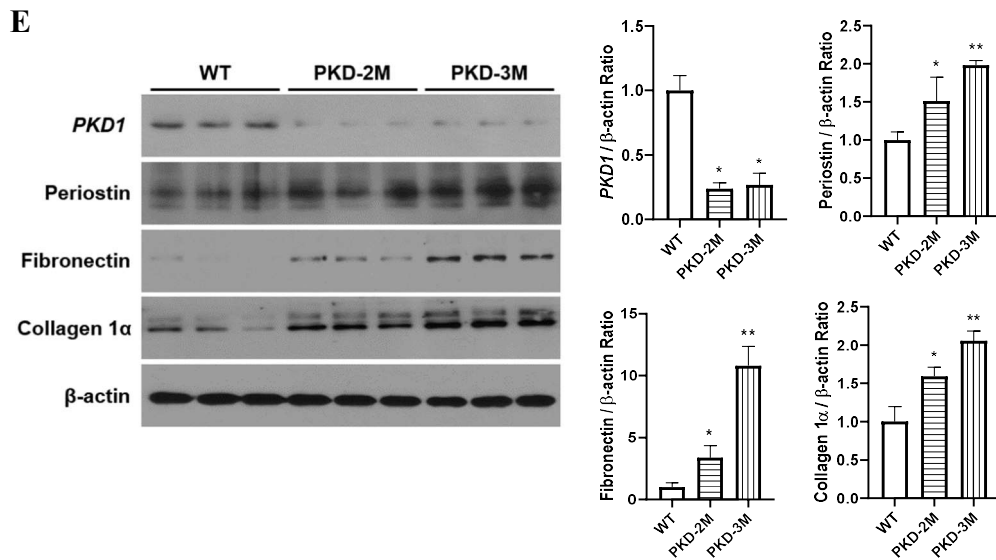


Figure 5. Kidney size, function, and mRNA and protein expression levels of fibrosis-related molecules in *PKD1* systemic-knockout mice. (A) Mean kidney weight to body weight (2KW/BW) ratio and kidney function parameter assessment in WT and *PKD1* systemic-knockout mice at postnatal 2- and 3-months. Increased kidney size, and higher levels of serum creatinine and BUN were observed in ADPKD mice, compared to that of WT mice. (B) Representative Periodic Acid-Schiff staining of histological kidney sections in WT and *PKD1* systemic-knockout mice at postnatal 2- and 3-months. Histological examination of the kidneys from 2- and 3-months old mice showed rapid progression of polycystic kidney disease. Bar = 20 μ m. (C) Cystic indices (%) in WT and *PKD1* systemic-knockout mice at postnatal 2- and 3-months. The cystic indices were significantly increased in ADPKD mice. (D) Relative mRNA level quantification of periostin, fibronectin, and type I collagen in WT and *PKD1* systemic-knockout mice. ADPKD mice showed significantly higher mRNA expression levels of periostin, fibronectin, and type I collagen, compared to that of WT mice. (E) Representative Western blotting analysis of protein expressions in WT and *PKD1* systemic-knockout mice at postnatal 2- and 3-months. ADPKD mice showed significantly higher protein expression levels of periostin, fibronectin, and type I collagen, compared to that of WT mice. Note: *, $P < 0.05$ vs. WT; #, $P < 0.05$ vs. PKD-2M; **, $P < 0.01$ vs. WT.

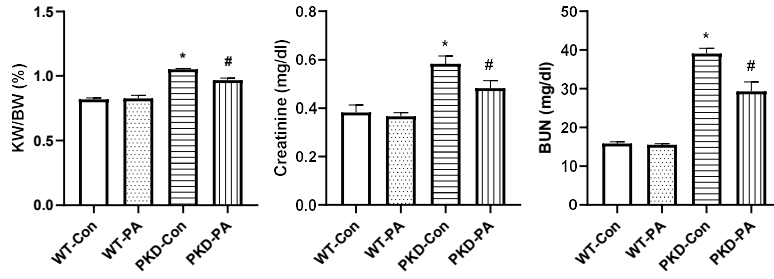
Abbreviations: KW, kidney weight; BW, body weight; BUN, blood urea nitrogen; WT, wild-type; ADPKD, autosomal dominant polycystic kidney disease.

3.6. Periostin-binding DNA aptamer treatment ameliorates cyst growth and fibrosis in *PKDI* systemic-knockout mice

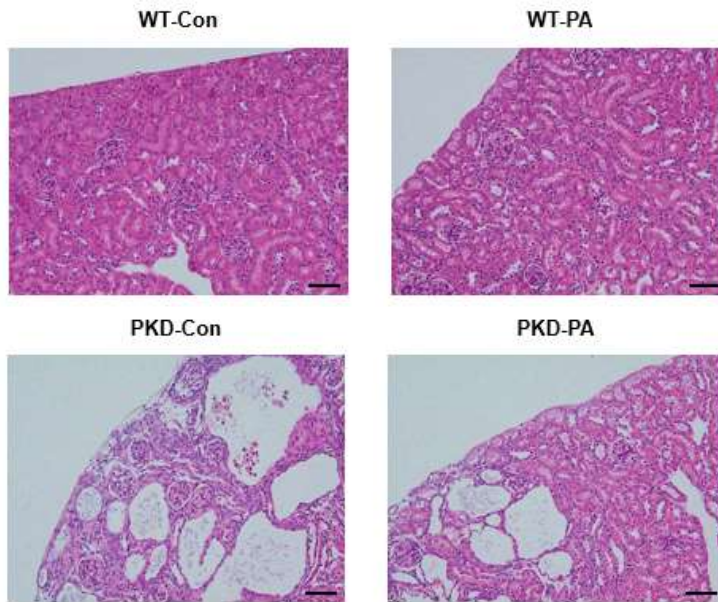
To validate the findings of the *in vitro* study, the *in vivo* effect of PA on cystogenesis in ADPKD was assessed using mouse models of ADPKD. The effect of PA treatment on kidney weight, kidney cystic area, and kidney function parameters, including BUN and serum creatinine, were investigated following treatment by intraperitoneal administration of PA (500 µg/kg/d) for 4 weeks in 4-week-old mice. As shown in **Figure 6A**, compared with WT mice, increases in kidney weight, serum creatinine and BUN levels in *PKDI* systemic-knockout mice were significantly abrogated by treatment with PA. Results of histological examinations of the kidneys of WT and *PKDI* systemic-knockout mice, before and after PA treatment, are shown in **Figure 6B**. PA treatment in *PKDI* systemic-knockout mice ameliorated cyst growth (**Figure 6B**), and significantly reduced the calculated cystic index (**Figure 6C**).

Administration of PA showed significant attenuation in the expression levels of periostin, fibronectin, and type I collagen mRNA and proteins (**Figures 6D and 6E**). *PKDI* systemic-knockout mice treated with PA exhibited significant attenuations in mRNA expressions of periostin, fibronectin, and type I collagen (**Figure 6D**). Similar findings were observed in the Western blot analysis (**Figure 6E**). These findings indicate that PA ameliorates cyst growth and fibrosis in ADPKD mice by abrogating expressions of periostin and fibrosis-related molecules.

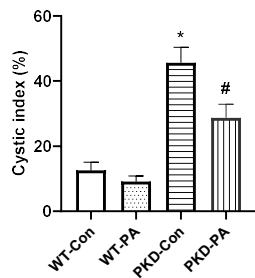
A



B



C



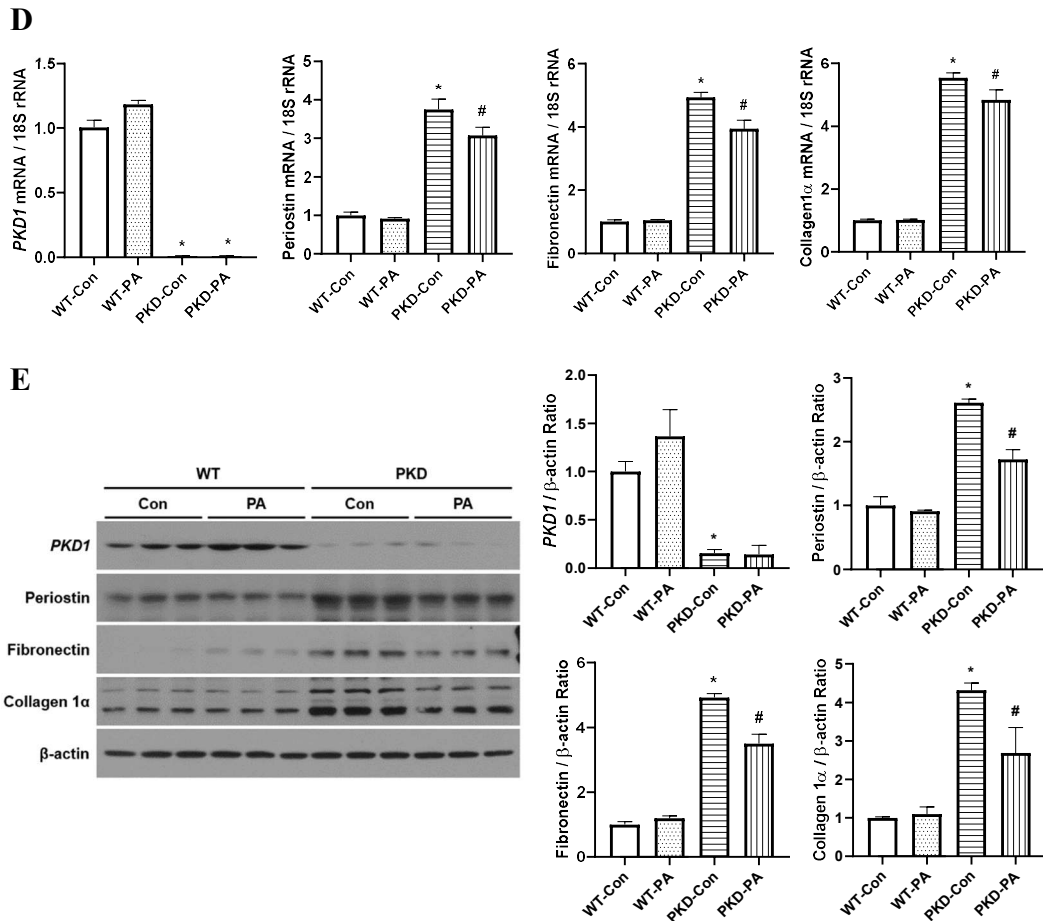


Figure 6. Periostin-binding DNA aptamer treatment ameliorates kidney cyst growth and attenuates fibrosis-related molecule expressions in *PKD1* systemic-knockout mice. (A)

Changes in mean kidney weight to body weight (KW/BW) ratio and kidney function parameters upon treatment of PA in WT and *PKD1* systemic-knockout mice. Treatment of ADPKD mice with PA significantly decreased kidney weight, serum creatinine and BUN levels. (B) Representative Periodic Acid-Schiff stains of histological kidney sections in WT and *PKD1* systemic-knockout mice treated with or without PA. Histological examination of the kidneys from WT and *PKD1* systemic-knockout mice treated with or without PA show that treatment with PA ameliorated kidney cyst growth. (C) Cystic indices (%) in WT and *PKD1* systemic-knockout mice treated with or without PA. The cystic indices were significantly decreased in ADPKD mice treated with PA.

Bar = 20 μm . (D) Periostin, fibronectin, and type I collagen mRNA levels in the kidneys of WT and *PKDI* systemic-knockout mice treated with or without PA. Periostin, fibronectin, and type I collagen mRNA expressions were significantly increased in ADPKD mice compared with WT mice. These increases were significantly abrogated by PA administration. (E) Representative Western blotting analysis of protein expressions in WT and *PKDI* systemic-knockout mice treated with or without PA. The protein levels of periostin, fibronectin, and type I collagen were significantly increased in ADPKD mice compared with WT mice. PA treatment significantly ameliorated these increases in protein levels in ADPKD mice.

Note: *, $P < 0.05$ vs. WT; #, $P < 0.05$ vs. PKD-control.

Abbreviations: WT, wild-type; con, control; PA, periostin-binding DNA aptamer; KW, kidney weight; BW, body weight; BUN, blood urea nitrogen; ADPKD, autosomal dominant polycystic kidney disease.

3.7. Periostin-binding DNA aptamer treatment attenuates integrin-linked kinase pathway activation in *PKDI* systemic-knockout mice kidneys

Finally, to determine whether the *in vivo* effects of PA in ADPKD mice was attributable to the attenuation of ILK pathway activation in the kidneys of *PKDI* systemic-knockout mice, WT and *PKDI* systemic-knockout mice treated with or without PA were examined for expression levels of phosphorylated-ILK, phosphorylated-AKT, phosphorylated-mTOR, and phosphorylated-ERK. As shown in **Figure 7**, the protein levels of phosphorylated-ILK, normalized to total ILK, was significantly higher in *PKDI* systemic-knockout mice relative to WT mice. PA treatment significantly abrogated these increases in *PKDI* systemic-knockout mice, as indicated by a decrease in the phosphorylated-ILK to ILK ratio upon PA treatment. Similar findings were observed for phosphorylated-AKT, phosphorylated-mTOR, and phosphorylated-ERK. These findings suggest that treatment with PA attenuates ILK pathway activation in the kidneys of *PKDI* systemic-knockout mice.

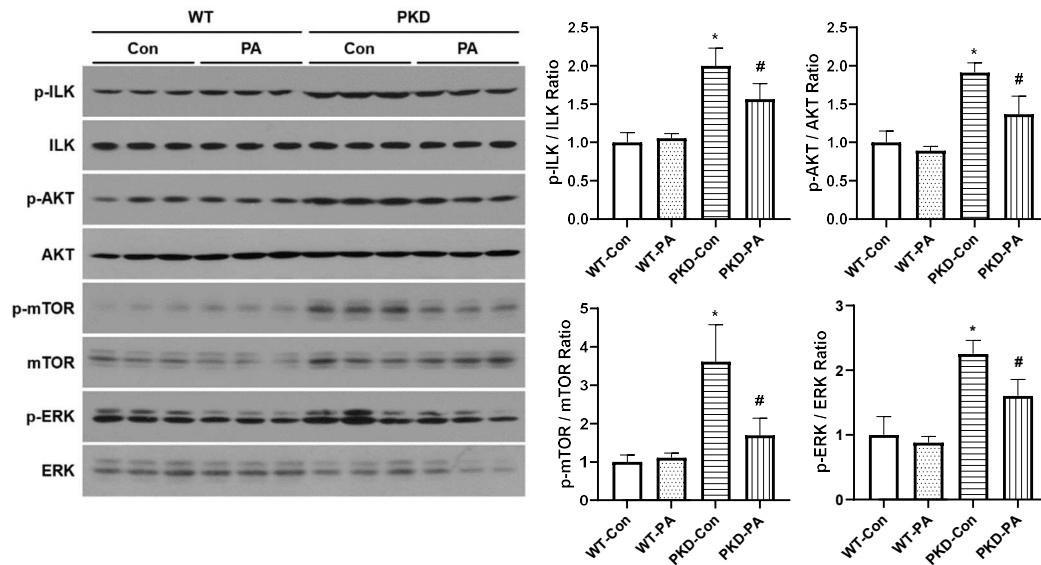


Figure 7. Periostin-binding DNA aptamer treatment attenuates ILK pathway activation in *PKD1* systemic-knockout mice kidneys. Representative Western blotting analysis of phosphorylated-ILK, phosphorylated-AKT, phosphorylated mTOR, and phosphorylated-ERK in the kidneys of *PKD1* systemic-knockout mice. The higher protein expression levels of phosphorylated-ILK, phosphorylated-AKT, phosphorylated-mTOR, and phosphorylated-ERK in the kidneys of *PKD1* systemic-knockout mice, compared to that of WT mice, was significantly abrogated upon treatment with PA. Levels of phosphorylated-ILK normalized to total ILK (p-ILK/ILK), phosphorylated-AKT normalized to total AKT (p-AKT/AKT), phosphorylated-mTOR normalized to total mTOR (p-mTOR/mTOR), and phosphorylated-ERK normalized to total ERK (p-ERK/ERK) were decreased upon PA treatment of *PKD1* systemic-knockout mice.

Note: *, $P < 0.05$ vs. WT; #, $P < 0.05$ vs. PKD-control.

Abbreviations: WT, wild-type; con, control; PA, periostin-binding DNA aptamer; ILK, integrin-linked kinase; AKT, protein kinase B; mTOR, mammalian target of rapamycin; ERK, extracellular signal-regulated kinase.

IV. DISCUSSION

The present study aimed to investigate the therapeutic effect of a DNA aptamer that binds specifically to periostin, a matricellular protein that is known to be overexpressed in human ADPKD cells compared with normal human kidney epithelial cells,³⁵ in ADPKD. This was investigated using WT9-7 cells in an *in vitro* model, and ADPKD mouse models *in vivo*. PA was observed to attach specifically to periostin expressed in WT9-7 cells without affecting cell viability. PA treatment successfully abrogated cyst growth and reduced the expressions of fibrosis-related molecules. This was accompanied by attenuation of ILK pathway activation, which is known to be an important mediator of periostin-induced ADPKD cell proliferation.³⁵ Furthermore, the effect of PA administration in ADPKD mouse models (*PKDI* systemic-knockout mice) was investigated. Intraperitoneal administration of PA led to reductions in kidney weight and kidney cyst growth, which was accompanied by attenuations in fibrosis-related molecule expressions and ILK pathway activation in the kidneys of *PKDI* systemic-knockout mice.

ADPKD is characterized by the formation and progressive expansion of numerous fluid-filled cysts that cause massively enlarged kidneys.⁵⁰ Kidney cysts are benign neoplasms that eventually cause kidney dysfunction through extensive loss of functioning nephrons and replacement of normal kidney parenchyma with fibrosis.⁵¹ Kidney cysts are formed due to not only intrinsic defects of ADPKD cells, but also due to factors secreted into the extracellular environment that contribute to cyst growth and development of interstitial fibrosis. In fact, when compared to normal human kidney cells, ADPKD cyst cells showed overexpression of several structural and soluble extracellular matrix components that included type I and type III collagen, periostin, and TGF- β . When periostin mRNA levels in cells derived from ADPKD and normal kidneys were observed, periostin mRNA expression was found to be 13.6-fold higher in ADPKD cells compared with normal kidney cells.³⁵ In line with these findings, when compared with HK-2 cells, WT9-7 cells exhibited higher mRNA and protein expression levels of periostin, fibronectin, and type I collagen.

Periostin belongs to a superfamily of TGF- β inducible proteins, and is mostly found in collagen-rich tissues such as periodontal ligaments, periosteum, and cardiac valves.²³ and is highly expressed in several tissues following injury.⁵² Regarding expression in the kidneys, periostin is expressed within the nephrogenic zone only during kidney development, but it is not expressed in normal adult

kidney.⁵³ However, in ADPKD, periostin is highly overexpressed by cyst-lining epithelial cells and accumulates within the ECM adjacent to cysts of ADPKD kidneys. Periostin is known to promote cyst epithelial cell proliferation and accelerate cyst growth *in vitro* but does not affect proliferation in normal human kidney cells. Indeed, when ADPKD cells were incubated with recombinant periostin, not only did the number of ADPKD cells increase by approximately 25%, compared to control, periostin also promoted cell cycle progression, and increased ADPKD cell proliferation 40% above control.³⁵ Similar to the findings of previous studies, WT9-7 cells that exhibited markedly higher levels of periostin mRNA and protein expressions levels, compared to that of HK-2 cells, showed notable cyst proliferation.

Previous studies have indicated that periostin acts as a ligand that binds to $\alpha V/\beta 3$ and $\alpha V/\beta 5$ integrins through its fascilin-1 domains.⁵⁴ This integrin is also involved in TGF- β overexpression and activation, which upregulates ECM production and promotes collagen cross-linking through activation of lysyl oxidase.^{55,56} Other pathways that stimulate cyst growth, such as the local renin-angiotensin system, chemokines, and other proinflammatory molecules, also promote TGF- β activity in ADPKD, and therefore potentially further stimulates the periostin/ αV -integrin/TGF- β circular chain.⁵⁷ Although the stimulation of the collagen fibrillogenesis by periostin maintains ECM integrity and influences the biomechanical properties of connective tissues,⁵⁸⁻⁶⁰ overexpression of periostin is known to be associated with organ fibrosis.⁶¹⁻⁶³ In the present study, there was a noticeable concomitant overexpression of structural ECM proteins that included fibronectin and type I collagen, further supporting the notion that periostin directly interacts with components of the ECM in ADPKD.²¹ Although PA treatment also appeared to downregulate the expression levels of periostin in this study, periostin expression *per se* is regulated by integrin activation; therefore, pharmacological inhibition of periostin-induced integrin activation by PA administration may have abrogated the expression of periostin.

Moreover, when considering the periostin/ αV -integrin/TGF- β positive feedback loop, and given the important role of integrin and TGF- β in the pathogenesis of kidney fibrosis and subsequent kidney function deterioration, interventions to regulate the deleterious effects of integrin or TGF- β could be considered. However, in a tamoxifen-inducible ADPKD mouse model, complete ILK knockout caused caspase-3-mediated anoikis, dilated cortical tubules with apoptotic cells in the lumens, interstitial fibrosis, and death of the mice by 10 weeks of age, suggesting that some degree of activity of the ILK pathway may be required for kidney cell survival and epithelium maintenance.

Although a small-molecule ILK inhibitor was shown to reduce kidney fibrosis in a model of obstructive nephropathy,⁶⁴ regulation of integrin via long-term use of an ILK inhibitor would need to be considered with caution. Similar to integrin, although TGF- β 1 is an important mediator in the pathogenesis of kidney fibrosis and subsequent kidney function deterioration, TGF- β 1 is also known to be involved in various physiological processes, such as wound recovery and immune reactions.^{65,66} Moreover, TGF- β 1 is located upstream of the TGF- β 1-induced fibrosis signaling cascade, and therefore, inhibition of TGF- β 1 is known to block various downstream intracellular signaling pathways that are critical for cell survival.^{67,68} In this regard, long-term use of a TGF- β 1 inhibitor may chronically suppress the immune system and stimulate loss of cell proliferation regulation.⁶⁹ Due to the important roles of integrin and TGF- β 1 in cell survival and intracellular signaling pathways, the fact that indirect regulation of these molecules via pharmacological inhibition of periostin abrogated the expression of fibrosis-related molecules in WT9-7 cells and ADPKD mice should be taken into account in this regard.

In the pathogenesis of ADPKD, several signaling pathways, including those regulated by cAMP, growth factors, B-Raf/mitogen-activated protein kinase/ERK, mTOR, AKT, and integrins have been implicated in aberrant cell proliferation and the relentless expansion of ADPKD cysts.^{15,35,70-76} Indeed, several previous studies have reported that inhibition of periostin downregulates mTOR by inactivation of the ILK pathway. In periostin knockout mice, phosphorylation levels of the ribosomal protein S6, a downstream target of the mTOR signaling pathway, was found to be significantly decreased.³⁶ Furthermore, mTOR is known to be activated downstream of ILK via AKT-dependent phosphorylation of tuberlin,⁷⁷ and therefore, an ILK-AKT-mTOR signaling axis may be an important mechanism underlying cyst cell proliferation in ADPKD cells. Consistent with the findings of previous studies, the increased protein expression levels of phosphorylated-ILK, phosphorylated-mTOR, phosphorylated-AKT, and phosphorylated-ERK in ADPKD cells and ADPKD mice, all of which were abrogated upon pharmacological inhibition of periostin by the administration of PA, further supports the presence of a signaling axis in the mechanism underlying periostin-stimulated cyst cell proliferation.

In this regard, inhibitors that target the mTOR pathway could abrogate cyst proliferation and subsequent kidney function deterioration in ADPKD. For example, in a ADPKD mouse model with Cre-mediated deletion of the *PKDI* gene, rapamycin treatment significantly improved cyst growth, fibrosis, proliferation, apoptosis, and overall kidney function, suggesting that mTOR inhibition

could benefit in the amelioration of the cystic phenotype in human ADPKD.¹⁷ However, in two randomized clinical trials involving patients with ADPKD, administration of sirolimus and everolimus, both of which are mTOR inhibitors, the rate of drug-specific adverse events, including leukopenia, thrombocytopenia, hyperlipidemia, oral mucositis, and diarrhea, was higher in the mTOR inhibitor treatment group.^{18,19} Furthermore, both drugs failed to slow polycystic kidney growth and subsequent progression of kidney function impairment. In contrast to mTOR inhibitors, DNA aptamers are single stranded oligonucleotides that are not only easy to modify for *in vivo* use, but also have low manufacturing costs and fewer side effects.⁷⁷ In the present study, a novel aptamer-based approach was used to inhibit periostin, which successfully ameliorated kidney cyst growth in ADPKD cells and ADPKD mice, and improved the kidney functions of ADPKD mice, by attenuating the expressions of fibrosis-related molecules and ILK pathway activation. Although the findings of this study suggest that DNA aptamers may also be effective in reducing kidney cyst growth in human ADPKD, clinical trials are warranted to establish the degree of potential clinical benefit and to weigh the risk-benefit of administering these therapeutic agents.

This study, however, is not without its limitations. Although *PKDI* systemic-knockout in young mice were induced by intraperitoneal injection of tamoxifen in mother mice on postnatal days 4–6, and subsequent transfer of this tamoxifen to the pups via breast feeding, the amount of tamoxifen delivered to the young mice may have varied. Furthermore, considering that the ADPKD mouse model used in this study utilized tamoxifen-inducible Cre mice, differences in the amount of tamoxifen actually delivered to the pups may have altered the degree of Cre-mediated *PKDI* gene disruption. Indeed, when the kidneys of young mice that received tamoxifen via breast-feeding from the tamoxifen-treated mother were compared to that of the mother mice that received tamoxifen individually and directly via oral administration, the kidneys of adult mice exhibited a two-fold higher expression of Cre, compared to that of young mice.⁷⁸ Therefore, the amount of tamoxifen intake in young mice via breastfeeding may have varied, and thus, leading to differences in efficiency of Cre-mediated *PKDI* gene disruption. Secondly, the HK-2 and WT9-7 cells used in *in vitro* experiments of this study both possess proximal tubular cell characteristics. However, the nephron-segment in which the majority of cyst proliferation occurred in *in vivo* was not determined in this study. Furthermore, although periostin is known to be produced by cyst-lining cells, which eventually leads to accumulation of periostin in ECM adjacent to the cysts and within cyst fluid,³⁵ further investigations into the specific nephron-segments that exhibited periostin overexpression

would have provided further insights into targeting periostin as a target protein in the development of therapeutic agents for ADPKD. Nevertheless, a global analysis of protein expression levels from the Kidney Interactive Transcriptomics (available from www.humphreyslab.com/SingleCell) indicates that transcript levels of periostin are expressed in all segments of the kidney tubules in adult human kidneys, and therefore PA treatment could potentially exert a broad effect across several nephron segments to slow cyst development. However, considering the differences in lifespan, metabolism, kidney anatomy, involved nephron-segment, and genetic backgrounds of different ADPKD mouse models, it would be difficult to perfectly recapitulate human ADPKD in *in vivo* studies. Finally, although the findings of this study indicated that PA treatment attenuated the expressions of fibrosis-related molecules, whether this translates to attenuations in the degree of fibrosis in the kidneys of ADPKD mice remains undetermined; therefore, further experiments that assess the changes in the degree of kidney fibrosis upon PA treatment are warranted.

V. CONCLUSION

In conclusion, the results of this study suggest that periostin acts as a key mediator of cyst proliferation in ADPKD, and treatment with a DNA aptamer that binds specifically to periostin may be considered as a modality to slow cyst growth and fibrosis in ADPKD. Although the findings of this study provide further evidence for the use of DNA aptamers and targeting of periostin in the treatment of ADPKD, clinical translation should be applied cautiously.

References

1. Bergmann C, Guay-Woodford LM, Harris PC, Horie S, Peters DJM, Torres VE. Polycystic kidney disease. *Nat Rev Dis Primers* 2018;4:50.
2. Caplan MJ. AMPK and polycystic kidney disease drug development: an interesting off-target target. *Front Med (Lausanne)* 2022;9:753418.
3. Willey C, Kamat S, Stellhorn R, Blais J. Analysis of nationwide data to determine the incidence and diagnosed prevalence of autosomal dominant polycystic kidney disease in the USA: 2013-2015. *Kidney Dis (Basel)* 2019;5:107-17.
4. Irazabal MV, Rangel LJ, Bergstralh EJ, Osborn SL, Harmon AJ, Sundsbak JL, et al. Imaging classification of autosomal dominant polycystic kidney disease: a simple model for selecting patients for clinical trials. *J Am Soc Nephrol* 2015;26:160-72.
5. Lanktree MB, Chapman AB. New treatment paradigms for ADPKD: moving towards precision medicine. *Nat Rev Nephrol* 2017;13:750-68.
6. Capuano I, Buonanno P, Riccio E, Rizzo M, Pisani A. Tolvaptan vs. somatostatin in the treatment of ADPKD: A review of the literature. *Clin Nephrol* 2022;97:131-40.
7. Harris PC, Torres VE. Genetic mechanisms and signaling pathways in autosomal dominant polycystic kidney disease. *J Clin Invest* 2014;124:2315-24.
8. Mekahli D, Parys JB, Bultynck G, Missiaen L, De Smedt H. Polycystins and cellular Ca²⁺ signaling. *Cell Mol Life Sci* 2013;70:2697-712.
9. Kim S, Nie H, Nesin V, Tran U, Outeda P, Bai CX, et al. The polycystin complex mediates Wnt/Ca(2+) signalling. *Nat Cell Biol* 2016;18:752-64.
10. Boletta A. Emerging evidence of a link between the polycystins and the mTOR pathways. *Pathogenetics* 2009;2:6.
11. Shillingford JM, Murcia NS, Larson CH, Low SH, Hedgepeth R, Brown N, et al. The mTOR pathway is regulated by polycystin-1, and its inhibition reverses renal cystogenesis in polycystic kidney disease. *Proc Natl Acad Sci USA* 2006;103:5466-71.
12. Baba M, Furihata M, Hong SB, Tessarollo L, Haines DC, Southon E, et al. Kidney-

- targeted Birt-Hogg-Dube gene inactivation in a mouse model: Erk1/2 and Akt-mTOR activation, cell hyperproliferation, and polycystic kidneys. *J Natl Cancer Inst* 2008;100:140-54.
13. Chen J, Futami K, Petillo D, Peng J, Wang P, Knol J, et al. Deficiency of FLCN in mouse kidney led to development of polycystic kidneys and renal neoplasia. *PLoS One* 2008:e3581.
 14. Tao Y, Kim J, Schrier RW, Edelstein CL. Rapamycin markedly slows disease progression in a rat model of polycystic kidney disease. *J Am Soc Nephrol* 2005;16:46-51.
 15. Wahl PR, Serra AL, Le Hir M, Molle KD, Hall MN, Wüthrich RP. Inhibition of mTOR with sirolimus slows disease progression in Han:SPRD rats with autosomal dominant polycystic kidney disease (ADPKD). *Nephrol Dial Transplant* 2006;21:598-604.
 16. Wu M, Wahl PR, Le Hir M, Wackerle-Men Y, Wuthrich RP, Serra AL. Everolimus retards cyst growth and preserves kidney function in a rodent model for polycystic kidney disease. *Kidney Blood Press Res* 2007;30:253-9.
 17. Zafar I, Belibi FA, He Z, Edelstein CL. Long-term rapamycin therapy in the Han:SPRD rat model of polycystic kidney disease (PKD). *Nephrol Dial Transplant* 2009;24:2349-53.
 18. Serra AL, Poster D, Kistler AD, Krauer F, Raina S, Young J, et al. Sirolimus and kidney growth in autosomal dominant polycystic kidney disease. *N Engl J Med* 2010;369:820-9.
 19. Walz G, Budde K, Mannaa M, Nürnberger J, Wanner C, Sommerer C, et al. Everolimus in patients with autosomal dominant polycystic kidney disease. *N Engl J Med* 2010;363:830-40.
 20. Perico N, Antiga L, Caroli A, Ruggenti P, Fasolini G, Cafaro M, et al. Sirolimus therapy to halt the progression of ADPKD. *J Am Soc Nephrol* 2010;21:1031-40.
 21. Kudo A. Periostin in fibrillogenesis for tissue regeneration: periostin actions inside and outside the cell. *Cell Mol Life Sci* 2011;68:3201-7.

22. Takayama G, Arima K, Kanaji T, Toda S, Tanaka H, Shoji S, et al. Periostin: a novel component of subepithelial fibrosis of bronchial asthma downstream of IL-4 and IL-13 signals. *J Allergy Clin Immunol* 2006;118:98-104.
23. Norris RA, Damon B, Mironov V, Kasyanov V, Ramamurthi A, Moreno-Rodriguez R, et al. Periostin regulates collagen fibrillogenesis and the biomechanical properties of connective tissues. *J Cell Biochem* 2007;101:695-711.
24. Bao S, Ouyang G, Bai X, Huang Z, Ma C, Liu M, et al. Periostin potently promotes metastatic growth of colon cancer by augmenting cell survival via the Akt/PKB pathway. *Cancer Cell* 2004;5:329-39.
25. Gillan L, Matei D, Fishman DA, Gerbin CS, Karlan BY, Chang DD. Periostin secreted by epithelial ovarian carcinoma is a ligand for alpha(V)beta(3) and alpha(V)beta(5) integrins and promotes cell motility. *Cancer Res* 2002;62:5358-64.
26. Lindner V, Wang Q, Conley BA, Friesel RE, Vary CPH. Vascular injury induces expression of periostin: implications for vascular cell differentiation and migration. *Arterioscler Thromb Vasc Biol* 2005;25:77-83.
27. Li G, Jin R, Norris RA, Zhang L, Yu S, Wu F et al. Periostin mediates vascular smooth muscle cell migration through the integrins alphavbeta3 and alphavbeta5 and focal adhesion kinase (FAK) pathway. *Atherosclerosis* 2010;208:358-65.
28. Shao R, Bao S, Bai X, Blanchette C, Anderson RM, Dang T, et al. Acquired expression of periostin by human breast cancers promotes tumor angiogenesis through up-regulation of vascular endothelial growth factor receptor 2 expression. *Mol Cell Biol* 2004;24:3992-4003.
29. Morra L, Rechsteiner M, Casagrande S, Luu VD, Santimaria R, Diener PA, et al. Relevance of periostin splice variants in renal cell carcinoma. *Am J Pathol* 2011; 179: 1513-21.
30. Baril P, Gangeswaran R, Mahon PC, Caulee K, Kocher HM, Harada T, et al. Periostin promotes invasiveness and resistance of pancreatic cancer cells to hypoxia-induced cell death:role of the beta4 integrin and the PI3k pathway. *Oncogene* 2007;26:2082-

- 94.
31. Riener MO, Fritzsche FR, Soll C, Pestalozzi BC, Probst-Hensch N, Clavien PA, et al. Expression of the extracellular matrix protein periostin in liver tumours and bile duct carcinomas. *Histopathology* 2010;56:600-6.
 32. Sasaki H, Lo KM, Chen LB, Auclair D, Nakashima Y, Moriyama S, et al. Expression of Periostin, homologous with an insect cell adhesion molecule, as a prognostic marker in non-small cell lung cancers. *Jpn J Cancer Res* 2001;92:869-73.
 33. Tischler V, Fritzsche FR, Wild PJ, Stephan C, Seifert HH, Riener MO, et al. Periostin is up-regulated in high grade and high stage prostate cancer. *BMC Cancer* 2010;10:273.
 34. Kudo Y, Ogawa I, Kitajima S, Kitagawa M, Kawai H, Gaffney PM, et al. Periostin promotes invasion and anchorage-independent growth in the metastatic process of head and neck cancer. *Cancer Res* 2006;66:6928–35.
 35. Wallace DP, Quante MT, Reif GA, Nivens E, Ahmed F, Hempson SJ, et al. Periostin induces proliferation of human autosomal dominant polycystic kidney cells through alphaV-integrin receptor. *Am J Physiol Renal Physiol* 2008;295:F1463-71.
 36. Wallace DP, Corey W, Savinkova L, Nivens E, Reif GA, Pinto CS, et al. Periostin promotes renal cyst growth and interstitial fibrosis in polycystic kidney disease. *Kidney Int* 2014;85:845-54.
 37. Raman A, Reif GA, Dai Y, Khanna A, Li X, Astleford L, et al. Integrin-linked kinase signaling promotes cyst growth and fibrosis in polycystic kidney disease. *J Am Soc Nephrol* 2017;28:2708-19.
 38. Lee K, Boctor S, Barisoni LMC, Gusella GL. Inactivation of integrin- β 1 prevents the development of polycystic kidney disease after the loss of polycystin-1. *J Am Soc Nephrol* 2015;26:888-95.
 39. Song KM, Lee S, Ban C. Aptamers and their biological applications. *Sensors* 2012;12:612-31.
 40. Keefe AD, Pai S, Ellington A. Aptamers as therapeutics. *Nat Rev Drug Discov* 2010;5:37-50.

41. Apte RS. Pegatanib sodium for the treatment of age-related macular degeneration. *Expert Opin Pharmacother* 2008;9:499-508.
42. Held DM, Kissel JD, Patterson JT, Nickens DG, Burke DH. HIV-1 inactivation by nucleic acid aptamers. *Front Biosci* 2006;11:89-112.
43. Lee YJ, Kim IS, Park SA, Kim Y, Lee JE, Noh DY, et al. Periostin-binding DNA aptamer inhibits breast cancer growth and metastasis. *Mol Ther* 2013;21:1004-13.
44. Um JE, Park JT, Nam BY, Lee JP, Jung JH, Kim Y, et al. Periostin-binding DNA aptamer treatment attenuates renal fibrosis under diabetic conditions. *Sci Rep* 2017;7:8490.
45. Nam BY, Park JT, Kwon YE, Lee JP, Jung JH, Kim Y, et al. Periostin-binding DNA aptamer treatment ameliorates peritoneal dialysis-induced peritoneal fibrosis. *Mol Ther Nucleic Acids* 2017;7:396-407.
46. Davies DR, Gelinis AD, Zhang C, Rohloff JC, Carter JD, O'Connell D, et al. Unique motifs and hydrophobic interactions shape the binding of modified DNA ligands to protein targets. *Proc Natl Acad Sci USA* 2012;109:19971-6.
47. Loghman-Adham M, Nauli SM, Soto CE, Kariuki B, Zhou J. Immortalized epithelial cells from human autosomal dominant polycystic kidney cysts. *Am J Physiol Renal Physiol* 2003;285:F397-412.
48. Nauli SM, Rossetti S, Kolb RJ, Alenghat FJ, Consugar MB, Harris PC, et al. Loss of polycystin-1 in human cyst-lining epithelia leads to ciliary dysfunction. *J Am Soc Nephrol* 2006;17:1015-25.
49. Mosmann T. Rapid colorimetric assay for cellular growth and survival: Application to proliferation and cytotoxicity assays. *J Immunol Methods* 1983;65:55-63.
50. Grantham JJ. 1992 Homer Smith Award. Fluid secretion, cellular proliferation, and the pathogenesis of renal epithelial cysts. *J Am Soc Nephrol* 1993;3:1841-57.
51. Wilson PD, Hreniuk D, Gabow PA. Abnormal extracellular matrix and excessive growth of human adult polycystic kidney disease epithelia. *J Cell Physiol* 1992;150:360-9.

52. Conway SJ, Izuhara K, Kudo Y, Litvin J, Markwald R, Ouyang G, et al. The role of periostin in tissue remodeling across health and disease. *Cell Mol Life Sci* 2014;71:1279-88.
53. Ito T, Suzuki A, Imai E, Horimoto N, Ohnishi T, Daikuhara Y, et al. Tornado extraction: a method to enrich and purify RNA from the nephrogenic zone of the neonatal rat kidney. *Kidney Int* 2022;62:763-9.
54. Kruzynska-Frejtag A, Wang J, Maeda M, Rogers R, Krug E, Hoffman S, et al. Periostin is expressed within the developing teeth at the sites of epithelial-mesenchymal interaction. *Dev Dyn* 2004;229:857-68.
55. Laczko R, Szauter KM, Jansen MK, Hollosi P, Muranyi M, Molnar J, et al. Active lysyl oxidase (LOX) correlates with focal adhesion kinase (FAK)/paxillin activation and migration in invasive astrocytes. *Neuropathol Appl Neurobiol* 2007;33:631-43.
56. Maruhashi T, Kii I, Saito M, Kudo A. Interaction between periostin and BMP-1 promotes proteolytic activation of lysyl oxidase. *J Biol Chem* 2010;285:13294-303.
57. Henderson NC, Arnold TD, Katamura Y, Giacomini MM, Rodriguez JD, McCarty JH, et al. Targeting of αv integrin identifies a core molecular pathway that regulates fibrosis in several organs. *Nat Med* 2013;19:1617-24.
58. Litvin J, Zhu S, Norris R, Markwald R. Periostin family of proteins: therapeutic targets for heart disease. *Anat Rec A Discov Mol Cell Evol Biol* 2005;287:1205-12.
59. Norris RA, Damon B, Mironov V, Kasyanov V, Ramamurthi A, Moreno-Rodriguez R, et al. Periostin regulates collagen fibrillogenesis and the biomechanical properties of connective tissues. *J Cell Biochem* 2007;101:695-711.
60. Norris RA, Moreno-Rodriguez R, Hoffman S, Markwald RR. The many facets of the matricellular protein periostin during cardiac development, remodeling, and pathophysiology. *J Cell Commun Signal* 2009;3:275-86.
61. Guerrot D, Dussaule JC, Mael-Ainin M, Xu-Dubois YC, Rondeau E, Chatziantoniou C, et al. Identification of periostin as a critical marker of progression/reversal of hypertensive nephropathy. *PLoS One* 2012;7:e31974.

62. Naik PK, Bozyk PD, Bentley JK, Popova AP, Birch CM, Wilke CA, et al. Periostin promotes fibrosis and predicts progression in patients with idiopathic pulmonary fibrosis. *Am J Physiol Lung Cell Mol Physiol* 2012;303:L1046-56.
63. Satirapoj B, Wang Y, Chamberlin MP, Dai T, LaPage J, Phillips L, et al. Periostin: novel tissue and urinary biomarker of progressive renal injury induces a coordinated mesenchymal phenotype in tubular cells. *Nephrol Dial Transplant* 2012;27:2702-11.
64. Li Y, Tan X, Dai C, Stolz DB, Wang D, Liu Y. Inhibition of integrin-linked kinase attenuates renal interstitial fibrosis. *J Am Soc Nephrol* 2009;20:1907-18.
65. Schiller M, Javelaud D, Mauviel A. TGF-beta-induced SMAD signaling and gene regulation: consequences for extracellular matrix remodeling and wound healing. *J Dermatol Sci* 2004;35:83-92.
66. Wang W, Huang XR, Li AG, Liu F, Li JH, Truong LD, et al. Signaling mechanism of TGF-beta1 in prevention of renal inflammation: role of Smad7. *J Am Soc Nephrol* 2005;16:1371-83.
67. Viñals F, Pouyssegur J. Transforming growth factor beta1 (TGF-beta1) promotes endothelial cell survival during in vitro angiogenesis via an autocrine mechanism implicating TGF-alpha signaling. *Mol Cell Biol* 2001;21:7218-30.
68. Brionne TC, Tesseur I, Masliah E, Wyss-Coray T. Loss of TGF-beta 1 leads to increased neuronal cell death and microgliosis in mouse brain. *Neuron* 2003;40:1133-45.
69. Biernacka A, Dobaczewski M, Frangogiannis NG. TGF- β signaling in fibrosis. *Growth Factors* 2011;29:196-202.
70. Qin S, Taglienti M, Nauli SM, Contrino L, Takakura A, Zhou J, et al. Failure to ubiquitinate c-Met leads to hyperactivation of mTOR signaling in a mouse model of autosomal dominant polycystic kidney disease. *J Clin Invest* 2010;120:3617-28.
71. Torres VE, Boletta A, Chapman A, Gattone V, Pei Y, Qian Q, et al. Prospects for mTOR inhibitor use in patients with polycystic kidney disease and hamartomatous diseases. *Clin J Am Soc Nephrol* 2010;5:1312-29.

72. Wallace DP. Cyclic AMP-mediated cyst expansion. *Biochim Biophys Acta* 2011;1812:1291-300.
73. Yamaguchi T, Hempson SJ, Reif GA, Hedge AM, Wallace DP. Calcium restores a normal proliferation phenotype in human polycystic kidney disease epithelial cells. *J Am Soc Nephrol* 2006;17:178-87.
74. Yamaguchi T, Nagao S, Wallace DP, Belibi FA, Cowley BD, Pelling JC, et al. Cyclic AMP activates B-Raf and ERK in cyst epithelial cells from autosomal-dominant polycystic kidneys. *Kidney Int* 2003;63:1983-94.
75. Yamaguchi T, Wallace DP, Magenheimer BS, Hempson SJ, Grantham JJ, Calvet JP. Calcium restriction allows cAMP activation of the B-Raf/ERK pathway, switching cells to a cAMP-dependent growth-stimulated phenotype. *J Biol Chem* 2004;279:40419-30.
76. Belibi F, Ravichandran K, Zafar I, He Z, Edelstein CL. mTORC1/2 and rapamycin in female Han:SPRD rats with polycystic kidney disease. *Am J Physiol Renal Physiol* 2011;300:F236-44.
77. Brody EN, Gold L. Aptamers as therapeutic and diagnostic agents. *J Biotechnol* 2000;74:5-13.
78. Lantinga-van Leeuwen IS, Leonhard WN, van der Wal A, Breuning MH, de Heer E, Peters DJ. Kidney-specific inactivation of the Pkd1 gene induces rapid cyst formation in developing kidneys and a slow onset of disease in adult mice. *Hum Mol Genet* 2007;16:3188-96.

Abstract in Korean

다낭성 신종에 있어서 periostin 특이 aptamer의 치료 효과 평가

배경: 상염색체우성 다낭신 (이하 다낭성 신종)은 신장이 다수의 낭종을 생성하여 결국 신장 기능이 저하되는 유전성 신질환이다. Periostin 은 다낭성 신종의 낭종을 둘러싸는 상피 세포에서 정상 세노관 세포에서 발현되는 양에 비해 과도하게 발현되는 세포 기질 단백질이다. Periostin 은 다낭성 신종 낭종 주변의 세포 외 기질에 축적되어, $\alpha V/\beta 3$, $\alpha V/\beta 5$ 인테그린 리간드에 결합하여 인테그린 연결 키나제 (ILK) 활성화를 통해 단백질 키나제 B (AKT)/mTOR 신호전달 경로를 상향 조절한다. aptamer는 표적 단백질에 특이적으로 결합함으로써 특정 타겟 단백질의 활성을 억제할 수 있는 올리고뉴클레오타이드이다. 본 연구에서는 다낭성 신종에서 periostin 에 특이적으로 결합하는 DNA aptamer (PA)의 치료 효과를 평가하였다.

방법: 체외 실험으로, PA 로 처리된 WT9-7 세포에서의 periostin 및 섬유증 관련 분자들의 mRNA 및 단백질 발현 정도의 변화와 ILK 경로 활성화 정도의 변화에 대해 평가하였다. PA 로 치료한 WT9-7 세포와 대조군의 낭종 크기들을 측정하여 낭종 성장을 비교하였다. 체내 실험에서, *PKDI* 전신적 녹아웃 쥐를 다낭성 신종 모델로 사용하였다. 8주 및 12주령 쥐들은 신장 낭종들의 성장을 관찰하기 위해 희생하였다. 쥐들은 출생 후 4주부터 총 4주간 복강 내 삼투 펌프를 통해 대조약 또는 PA 를 복강 내로 투여 받았다. PA 처리 후 낭종성 질환 매개 변수들의 변화, periostin 및 섬유증 관련 분자들의 발현 수준들의 변화, 그리고 ILK 경로 활성화 정도의 변화를 평가하였다.

결과: 형광 활성화 세포 분류 분석에서 Cy3로 표지된 PA 가 WT9-7 세포에 성공적으로 결합하는 것을 확인하였다. WT9-7 세포에 PA (200 nM)를 처리하면 periostin, fibronectin 및 제1형 콜라겐을 포함한 섬유증 관련 분자들의 mRNA 및 단백질 발현이 억제되었고, 세포 생존도에는 영향을 미치지 않았다. 이는 WT9-7

세포에서 ILK 에 의해 활성화된 AKT/mTOR 신호 경로의 억제를 통해 매개되었으며, 이는 PA 처리 시 인산화-ILK, 인산화-AKT, 인산화-mTOR 및 인산화-ERK 의 발현량 감소로 나타났다. PA 는 WT9-7 세포의 세포 성장을 감소시켰다. 체내 연구에서는 다낭성 신종 쥐들의 신장에서 형태학적인 낭종 변화가 8주부터 관찰되었다. 출생 후 4주부터 4주간 *PKD1* 전신적 녹아웃 쥐들에서 PA (500 μ g/kg/일)를 처리한 결과, 낭종 성장이 감소하였고 섬유증 관련 분자들의 발현이 억제되었다. 이러한 효과는 *PKD1* 전신적 녹아웃 쥐들의 신장에서 ILK 경로 활성화의 억제와 동반되었다.

결론: 본 연구는 periostin이 다낭성 신종에서 낭종 증식의 핵심 매개체로 작용하며, periostin에 특이적으로 결합하는 DNA 압타머 치료가 다낭성 신종에서 낭종의 성장과 섬유증을 늦추는 방법으로 고려될 수 있다.

핵심되는 말 : 상염색체우성 다낭신; periostin; 압타머; 뉴클레오타이드; 낭종.